Solvent reorganization energy of electron-transfer reactions in polar solvents

Dmitry V. Matyushov[a)]
Department of Chemistry and Biochemistry and the Center for the Early Events in Photosynthesis, Arizona State University, Tempe, Arizona 85287-1604

(Received 26 September 2003; accepted 21 January 2004)

A microscopic theory of solvent reorganization energy in polar molecular solvents is developed. The theory represents the solvent response as a combination of the density and polarization fluctuations of the solvent given in terms of the density and polarization structure factors. A fully analytical formulation of the theory is provided for a solute of arbitrary shape with an arbitrary distribution of charge. A good agreement between the analytical procedure and the results of Monte Carlo simulations of model systems is achieved. The reorganization energy splits into the contributions from density fluctuations and polarization fluctuations. The polarization part is dominated by longitudinal polarization response. The density part is inversely proportional to temperature. The dependence of the solvent reorganization energy on the solvent dipole moment and refractive index is discussed. © *2004 American Institute of Physics.* [DOI: 10.1063/1.1676122]

I. INTRODUCTION

In the course of an electron-transfer (ET) reaction the center of localization of the transferred electron is shifted from the donor to the acceptor. This creates a difference electric field $\Delta\mathbf{E}_0(\mathbf{r})$ commonly represented by the ET (nonpoint) dipole formed by a positive charge on the donor and a negative charge on the acceptor (Fig. 1). The coupling of the ET dipole to electronic and nuclear degrees of freedom of the solvent is responsible for the thermodynamic and dynamic effects of the solvent on ET activation. The first solution for the problem of the solvent effect on ET energetics was proposed by Marcus.[1,2] His approach considers solvation of two isolated, oppositely charged spherical ions with radial symmetry of their electric fields. A finite distance between the positive and negative charges of the ET dipole is included through their Coulomb attraction.

The Marcus formulation, deceptive in its simplicity, includes an important physical assumption, that electronic transitions are activated by fluctuations of the longitudinal nuclear solvent polarization δP^L produced by thermally reorienting permanent dipoles of the solvent molecules. This notion connects the Marcus theory to the Born theory of ion solvation[3] and to earlier descriptions of large polarons and F centers in polar lattices.[4] In all these cases, the spherical symmetry of the field of a single charge is supplemented by equal spherical symmetry of the cavity carved in the dielectric, thus leading to a radial distribution of the polarization. Similarly, the Marcus formulation applies only to situations when both the equilibrium and nonequilibrium (activated state) polarizations of the solvent can be represented by solvent response to an effectively spherically symmetric field of the solute.

The longitudinal nature of the solvent response is reflected by the appearance of the longitudinal relaxation time τ^L in ET rate constants affected by solvent dynamics.[5–7] Also, time-resolved measurements of solvation dynamics indicate that τ^L is the appropriate relaxation time for the long-time portion of the solvation correlation functions.[8–10] In the static regime, the Pekar factor $c_0=1/\epsilon_\infty-1/\epsilon_s$ is a signature of the longitudinal nuclear polarization, where ϵ_∞ and ϵ_s are the high-frequency and static dielectric constants, respectively. The Marcus equation (superscript "M") for the solvent reorganization energy defines the characteristic energy scale of the effect of longitudinal polarization fluctuations on the donor–acceptor energy gap

$$\lambda_s^{\mathrm{M}}=c_0\mathcal{E}_0^L. \tag{1}$$

Here,

$$\mathcal{E}_0^L=(8\pi)^{-1}\int|\Delta\tilde{E}_0^L(\mathbf{k})|^2\frac{d\mathbf{k}}{(2\pi)^3} \tag{2}$$

is the electrostatic energy corresponding to the inverted-space longitudinal projection of the electric field $\Delta\tilde{\mathbf{E}}_0$ on the direction of the wave vector $\hat{\mathbf{k}}=\mathbf{k}/k$: $\Delta\tilde{E}_0^L(\mathbf{k})=(\hat{\mathbf{k}}\cdot\Delta\tilde{\mathbf{E}}_0)$. The Fourier transform

$$\Delta\tilde{\mathbf{E}}_0(\mathbf{k})=\int_\Omega\Delta\mathbf{E}_0(\mathbf{r})e^{i\mathbf{k}\cdot\mathbf{r}}d\mathbf{r} \tag{3}$$

is taken over the solvent volume Ω outside the donor–acceptor complex (DAC). The energy $\mathcal{E}_0^L$ is often called the geometric factor as it is solely determined by the shape of the DAC and the geometry of electron localization in the initial (donor) and final (acceptor) states.

The concept of longitudinal polarization most naturally appears in the inverted-space representation of the electrostatic fields.[6,11,12] The longitudinal component $\tilde{P}^L(\mathbf{k})=\hat{\mathbf{k}}\cdot\tilde{\mathbf{P}}(\mathbf{k})$ of the $\mathbf{k}$-space Fourier transform $\tilde{\mathbf{P}}(\mathbf{k})$ of the dielectric polarization is directly connected to the density of the external charge $\tilde{\rho}_0(\mathbf{k})$ by Maxwell's equation

a)Electronic mail: dmitrym@asu.edu

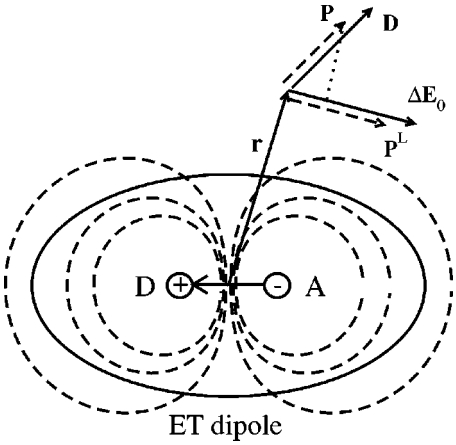

FIG. 1. ET dipole formed by a negative charge on the acceptor (A) and a positive charge on the donor (D). The dashed lines show equipotential surfaces of the ET dipole which cross the cavity surface (solid line). The dielectric displacement **D** is then nonequal to the source field $\Delta\mathbf{E}_0$. For that reason the projection of the solvent polarization **P** on the direction of the source field is not equal to $\mathbf{P}^L$ given by Eq. (5).

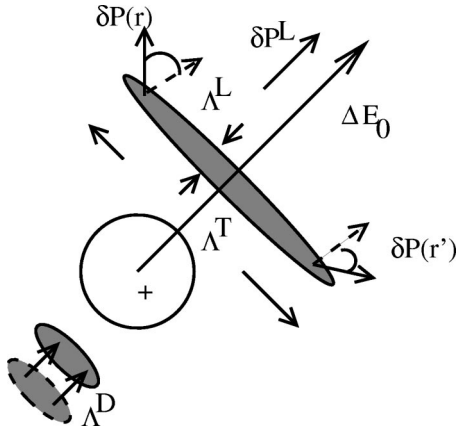

FIG. 2. Orientational and density fluctuations around a spherical ion. Λ^L, Λ^T, and Λ^D denote the longitudinal, transverse, and density correlation lengths, respectively (see the text).

$$\tilde{P}^L(\mathbf{k}) = \left(1 - \frac{1}{\epsilon_s}\right)\frac{i\tilde{\rho}_0(\mathbf{k})}{k}. \tag{4}$$

This connection substantially simplifies all the electrostatic calculations in cases when $\tilde{P}^L = \tilde{P}$. In the direct space, this condition implies that the polarization of the dielectric surrounding a solute can be directly connected to the vacuum source field:

$$\mathbf{P} = \mathbf{P}^L = \frac{1}{4\pi}\left(1 - \frac{1}{\epsilon_s}\right)\Delta\mathbf{E}_0. \tag{5}$$

This relation also implies that Maxwell's dielectric displacement **D** within the dielectric is equal to the source field $\Delta\mathbf{E}_0$:

$$\mathbf{D} = \Delta\mathbf{E}_0. \tag{6}$$

The free energy of solvation, F_{solv}, can then be easily calculated from the vacuum external field by integration of the electrostatic energy density over the volume occupied by the solvent:

$$F_{\text{solv}} = -\frac{1}{2}\int_\Omega \mathbf{D}(\mathbf{r})\cdot\mathbf{P}(\mathbf{r})d\mathbf{r} = -\frac{1}{8\pi}\left(1 - \frac{1}{\epsilon_s}\right)\int_\Omega \Delta E_0(\mathbf{r})^2 d\mathbf{r}. \tag{7}$$

As was recognized by Kharkats *et al.*[13] Eq. (6) is satisfied only when the boundary of the cavity cut off by the DAC from the solvent coincides with an equipotential surface of the charge distribution within the cavity. When this is not the case, the lines of the source field are not normal to the cavity surface resulting in $\mathbf{D} \neq \Delta\mathbf{E}_0$ (Fig. 1). The dielectric polarization is then determined by both the source charge and the apparent surface charge,[14] and Eq. (5) does not hold any more. In the direct-space representation, this means that dielectric displacement should be sought by solving the Poisson equation with the boundary conditions set up by the dielectric cavity. In the **k**-space description, this implies that the polarization is not solely given by the source charge distribution [Eq. (4)] and the transverse polarization component $\tilde{P}^T = |\tilde{\mathbf{P}} - \hat{\mathbf{k}}(\hat{\mathbf{k}}\cdot\tilde{\mathbf{P}})|$ contributes to the solvent response. It was argued that a cavity containing an ET dipole always crosses its equipotential surfaces (Fig. 1) and transverse polarization cannot be neglected.[13] Both the longitudinal and transverse components of the solvent polarization then affect the energy gap ΔE between the acceptor and donor electronic states. This symmetry change broadens the spectrum of solvent collective modes activating ET from purely longitudinal, as in the case of large polarons, to longitudinal, P^L, and transverse, P^T, polarization modes (Figs. 1 and 2).

The importance of both the longitudinal and transverse polarization modes is well recognized in current continuum formulations of the ET theory which search for a solution of the Poisson equation for the ET dipole in a cavity of arbitrary shape.[15–17] Indeed, the calculation of electrostatic energy of the ET dipole within ellipsoidal cavities shows that the solvent reorganization energy λ_s cannot be separated into a solvent (e.g., Pekar factor) and geometric ($\mathcal{E}_0^L$) factors. The dependence of λ_s on the solvent dielectric constant is entangled with the cavity shape.[18] Therefore, both longitudinal and transverse polarizations contribute to the electric field of the solvent interacting with solute's charges. At this point, the continuum electrostatic calculations come in contradiction to the original Marcus concept and studies of ET dynamics both pointing to the longitudinal polarization as the principal solvent mode driving electronic transitions.

The recent two decades have seen an increasing interest in the development of microscopic theories of ET reorganization.[19–29] Theoretical models are usually based on either liquid-state theories of solvation[19–24,29] or direct computer simulations of the reorganization energy[25,30] and ET free energy surfaces.[26–28,31] This development has recognized the fact that the coupling of macroscopic fluctuations of dipolar polarization to the ET dipole is not the only mechanism of ET activation, and other interaction potentials and molecular modes may be active as well. Two major extensions of the original Marcus concept have been suggested: (i) a distinction between rotational and translational modes of the solvent affecting ET activation[20,32] and solvation dynamics[33,34] and (ii) the role of higher solvent multi-

poles for reactions in weakly polar and nondipolar solvents.[21,22,30,35–37]

On short time scales of solvation dynamics, when long-range multipolar correlations are not yet established, both rotations and translations participate in purely ballistic motion.[33] The dynamics of solvent response due to translations and rotations becomes, however, distinctly different on diffusional time scales when the long-range orientational correlations become active.[34] Finally, in the static regime, when the time scale of the process of interest (k_{ET}^{-1} for ET, where k_{ET} is the ET rate constant) is much larger than the characteristic time scales of molecular motions, the difference in correlation lengths of the density (translations) and orientational (rotations) collective modes is reflected in a much stronger temperature dependence of the density component of the solvent reorganization energy.[20] The same is true not only for charge–dipole solute–solvent coupling, but also for other interaction potentials depending on the coordinates of the solvent molecules (induction and dispersion forces).[38,39] Fluctuations of all these potentials, caused by density fluctuations of the solvent, lead to a pronounced temperature dependence of λ_s. The entropy of solvent reorganization is thus dominated by short-range density fluctuations and not by long-range orientational fluctuations. The total reorganization entropy is positive as confirmed by experiment,[40–44] in contrast to a negative entropy predicted by dielectric cavity models.

An account for higher solvent multipoles, in particular for solvent quadrupoles coupled to the gradient of the solute electric field, is necessary for solvents composed of molecules with small or zero dipole moment.[21,22,35,36] This modification of the theory goes necessarily beyond dielectric models since the dielectric constant reflects molecular quadrupoles only indirectly (through the Kirkwood factor).[45,46] The charge–quadrupole interaction decays faster with the distance than the charge–dipole interaction. The relative importance of quadrupole moments in solvents with nonzero dipoles depends therefore on the solute size. For commonly large donor and acceptor units employed in ET studies, the quadrupolar contribution to the solvent reorganization energy is small in all but nondipolar solvents, and the quadrupolar solvation energy can be safely dropped for ET in even weakly polar solvents.[30] We therefore focus in this study on dipolar polarization fluctuations, reserving a relatively narrow class of nondipolar solvents to future work.

The present state of the problem of calculating the solvent reorganization energy in polar solvents may be summarized as follows. Dielectric continuum models offer significant flexibility in treating molecular solutes of complex geometries. A solution of the Poisson equation for a molecular cavity includes both the longitudinal and transverse polarization components. Procedures of defining cavities are, however, ambiguous and the calculation results are very sensitive to the choice of the dielectric cavity. In addition, it is not clear whether the equal account of two types of polarization by the Poisson equation is consistent with quite different time and length scales of these two modes on the microscopic level (Fig. 2). On the other side of the theoretical spectrum, molecular solvation theories incorporate a more realistic description of molecular dynamics and thermodynamics. Existing models are, however, limited in their ability to treat large solutes of complex molecular shape. Both the longitudinal and transverse polarization components were included in the solvent response for a spherical dipolar solute.[36,47] That model has been used to calculate steady-state optical band shapes for dipolar chromophores in a broad range of solvent polarities[30] and has been applied to calculate entropies of ET activation.[37,48] The effective radius of the solute is not, however, specified in the model and should be fitted to some experimental observable; the Stokes shift[30,42] and the equilibrium energy gap[37] have been used in recent applications. The transverse polarization is often neglected in microscopic models of the energetics[20–22] and dynamics[6] of ET. It is not included in the RISM calculations[21,22] due to the way the RISM approximation is formulated.[49] The combination of limitations in treating solute molecular geometry with neglect of some important collective polarization modes present in molecular solvents obviously narrows the range of applications of molecular solvation models. The development of an effective algorithm applicable to an arbitrary geometry of the DAC with full account of solvent polarization modes is a pressing need for applications, especially in the realm of redox chemistry of biopolymers. This paper presents the first step in this direction.

Various levels of complexity may be chosen for molecular modeling of the solvent effect. Realistic intermolecular potentials with partial molecular and atomic charges are often used in computer simulations. These approaches provide a very detailed picture of the local solute–solvent structure. These models are, however, hard to employ in formal theories. Furthermore, a still existing ambiguity of treating long-range Coulomb forces in computer simulations, especially at infinite dilution of large solutes common for biological applications, leaves open the question of the ability of finite-size simulations to grasp the long-range polarization structure of the solvent around a molecular solute. On the other hand, a tremendous success of continuum models in treating the Gibbs energy of solvation[50] suggests that a substantial portion of significant physics is accounted for even on the continuum level of the theory. The dielectric continuum approach fails to describe short-range solvation effects reflected by such properties as the entropy of solvation,[20,51] quadrupolar solvation,[21,22,30,35–37,46] and specific interactions.[52] However, the formalism of response functions,[53–56] providing a reduced description of the complex molecular problem, is a valuable component of the continuum approach which can be extended to include various molecular modes and molecular dimensions. This is the basic approach adopted in this paper. The formalism for the calculation of the reorganization energy is given in terms of k-dependent density[57] and polarization[58,59] structure factors of the solvent which are incorporated into the theory to form the nonlocal polarity response functions depending on both the solvent and solute geometry. For convenience, we will refer to the present formulation as to the nonlocal response function theory (NRFT). The analytical calculations for

model solute geometries and computer simulations are performed for the model solvent of multipolar hard spheres.

The model of polarizable hard spheres with centered molecular multipoles has the desired universality in a sense that it may be parametrized to describe a broad list of molecular solvents[60–63] on the one hand and incorporates the main thermal molecular motions of real solvents—rotations and translations—on the other. An additional advantage is that the solvent molecular polarizability, which is often very expensive for computer simulations,[64,65] is incorporated through a renormalized solvent dipole.[45,66–68] The spherical approximation for molecular cores of the solvent molecules may seem to be an oversimplification, but there are strong arguments for its ability to account for nonspecific solvent effects on chemical thermodynamics and solvation.[69] Recent applications of the model have demonstrated its ability to accurately describe activation[37,48,70] and spectroscopy[30] of charge-transfer transitions. Although the calculations and simulations are done here for the model of dipolar solvent molecules, the formalism is not limited by this assumption. The theory is formulated in terms of density and polarization structure factors of the pure solvent and those for an arbitrary molecular solvent can be used in the calculations.

The results of microscopic calculations are compared throughout the paper to the continuum limit which follows from the NRFT when k dependence is neglected in the solvent response functions. The notion of continuum solvation applies to the *dielectric continuum* description as first formulated by Born,[3] Onsager,[71] and Kirkwood.[72] A few recent *continuum* solvation models[73–75] incorporate molecular properties which are not reflected by the static and high-frequency dielectric constants of the solvent. These continuum approximations are not considered here as the NRFT includes only dielectric continuum as its limiting case.

The rest of the paper is organized as follows: The next section provides a compilation of critical properties of the solvent reorganization energy illustrated by the results from Monte Carlo (MC) simulations. This compilation sets up a list of requirements which an accurate analytical model of solvent reorganization should meet. The theory development starts with the instantaneous free energies depending on the nuclear configuration of the system as given in Sec. III. The formulation of the theory of solvent reorganization is presented in Sec. IV. This is followed by the development of an analytical approximation to calculate the polarization structure factors of a pure polar solvent in Sec. V. A description of the numerical algorithm and a comparison between the analytical theory and simulations are presented in Sec. VI. The paper concludes with a short summary in Sec. VII.

II. CONCEPTUAL FORMULATION

A. Solvent reorganization energy in the linear response approximation

Radiationless transitions are activated by thermal nuclear fluctuations creating the resonance of the donor and acceptor electronic levels. The rate constant of ET, k_{ET}, is proportional to the probability of a nuclear configuration leading to zero energy gap $\Delta E=0$ between the donor and acceptor electronic states,

$$k_{\mathrm{ET}} \propto P_i(0). \tag{8}$$

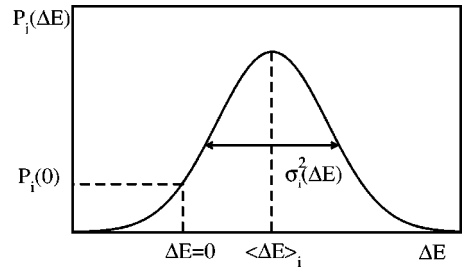

FIG. 3. Distribution function of energy gaps between the donor and acceptor electronic energy levels. $\langle \Delta E\rangle_i$ and σ_i^2 denote, respectively, the first and second cumulants of the distribution function.

The probability distribution $P_i(\Delta E)$ for the initial $(i=1)$ and final $(i=2)$ states of the transferred electron is fully characterized by its infinite cumulant series. Only two first cumulants—the average vertical gap $\langle \Delta E\rangle_i$ and the variance $\sigma_i^2(\Delta E)$—are nonzero when $P_i(\Delta E)$ is a Gaussian distribution (Fig. 3). For classical nuclear modes of the solvent, the variance is commonly factored into the temperature and classical solvent reorganization energy, λ_i, terms:[76]

$$\sigma_i(\Delta E)^2 = 2k_BT\lambda_i, \quad \lambda_i = (\beta/2)\langle(\delta\Delta E)^2\rangle_i. \tag{9}$$

Here $\beta=1/k_BT$, k_B is Boltzmann's constant, and T is temperature; $\langle\cdots\rangle_i$ denotes an equilibrium ensemble average in the ith state. The factorization of Eq. (9), characteristic of the classical limit of the fluctuation–dissipation theorem,[77] conveniently separates the temperature factor from the reorganization energy. The latter is assumed to depend weakly on temperature.

The molecular origin of a nonzero variance $\sigma_i^2(\Delta E)$ is in thermal fluctuations of the solute–solvent interaction potential which is often given by a sum of pairwise interactions,

$$V_i = \sum_j v_i(j). \tag{10}$$

Here $j=\{\mathbf{r}_j,\omega_j\}$ stands for the coordinates and Euler angles of the jth solvent molecule and the sum runs over the N solvent molecules. Thermal fluctuations of $\Delta V=V_2-V_1$ in $\Delta E=E_2-E_1$ are responsible for a nonzero value of the variance $\sigma_i(\Delta E)$. The corresponding reorganization energy can be split into a sum of a single-molecule (one probe solvent molecule) and two-molecule (two probe solvent molecules) contributions,

$$\lambda_i = \lambda_i^{\mathrm{I}} + \lambda_i^{\mathrm{II}}. \tag{11}$$

Here,

$$\lambda_i^{\mathrm{I}} = (\beta/2)\sum_j \langle(\delta\Delta v(j))^2\rangle_i, \tag{12}$$

$$\lambda_i^{\mathrm{II}} = (\beta/2)\sum_{j\neq k} \langle \delta\Delta v(j)\,\delta\Delta v(k)\rangle_i, \tag{13}$$

and $\Delta v(j)=v_2(j)-v_1(j)$.

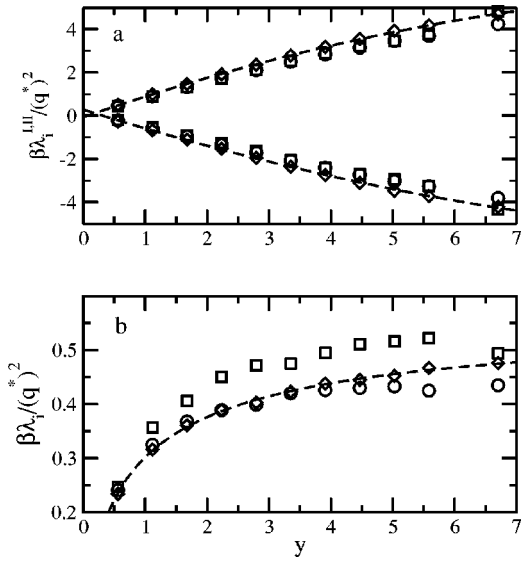

FIG. 4. (a) One-molecule (upper set of points) and two-molecule (lower set of points) contributions to the solvent reorganization energy. (b) Solvent reorganization energy vs the dipolar density [Eq. (15)]. Points refer to simulations in dipolar (circles and diamonds, $Q^*=0$) and dipolar–quadrupolar [squares, $(Q^*)^2=0.5$] solvents of varying dipolar strength. Reorganization energies λ_i are obtained from the variance of the solute–solvent difference potential measured on solvent configurations in equilibrium with a neutral diatomic D–A ($i=1$, circles and squares) and in equilibrium with a charged diatomic D^+-A^- ($i=2$, diamonds); $\rho^*=0.8$, $R_D=R_A=0.9\sigma$, and $R=2R_D$. The dashed lines are regressions drawn through the diamond points. The reduced charge $q^*=11.87$ is defined by Eq. (A2).

In polar molecular liquids, the one-particle and two-particle terms in λ_i are essentially compensating each other.[78] The resultant reorganization energy λ_i usually constitutes about 10% of λ_i^{I} or λ_i^{II} as is illustrated in Fig. 4(a). Figure 4 shows the results of MC simulations for a model ET reaction between two spherical reactants at a distance equal to the sum of their radii (contact configuration). The donor and acceptor are immersed in a liquid of hard-sphere (HS) molecules with point dipoles (diamonds and spheres in Fig. 4) and with point dipoles and axial quadrupoles (squares in Fig. 4). The details of simulations and the actual simulation results are given in Appendix A. For the calculations presented in Fig. 4 the pairwise solute–solvent interaction potential is the interaction of the electric field of the solute $\mathbf{E}_{0i}$ with the solvent point dipole,

$$v_i(j)=-\mathbf{m}_j\cdot\mathbf{E}_{0i}(\mathbf{r}_j). \tag{14}$$

The interaction of the solute with the solvent quadrupole moment is not explicitly considered. Solvent quadrupoles are introduced here for a more realistic modeling of dipolar correlations in polar solvents (see below).[46] All results in this paper refer to the interaction of the solute charges with dipolar polarization only.

Diamonds in Fig. 4 represent simulations in equilibrium with the charged state of the solute, D^+-A^-; the circles and squares correspond to a neutral diatomic, D–A. In both cases, the reorganization energies are obtained as the variance of the difference potential ΔV according to Eq. (9). Since the initial state is a nonpolar diatomic, $\Delta V=\Sigma_j v_2(j)$, where $v_2(j)$ is given by Eq. (A1). The reorganization energy components $\lambda_i^{\mathrm{I,II}}$ [Fig. 4(a)] and the total reorganization energies λ_i [Fig. 4(b)] are plotted in Fig. 4 against the dipolar strength,

$$y=(4\pi/9)\beta\rho m^2, \tag{15}$$

where ρ is the solvent number density and m is the solvent permanent dipole. Below we also use the reduced dipole moment $(m^*)^2=\beta m^2/\sigma^3$ independent of the bulk density, where σ is the diameter of the solvent molecules. The results of computer simulations are presented in this section to illustrate the main qualitative features of ET reorganization in polar solvents. A quantitative analysis is postponed to Sec. IV.

Figure 4 shows that, within simulation uncertainties, the reorganization energies for D–A and D^+-A^- solutes are equal. This means that the linear response approximation (LRA) is valid for solvation of charges in multipolar solvents within the range of studied polarities. The LRA assumes that the electric field of the solvent polarization is linear in solute's charges leading to the reorganization energy independent of the electronic state,

$$\lambda_1=\lambda_2=\lambda_s. \tag{16}$$

This is the Marcus picture of ET activation in terms of two intersecting parabolas with equal curvatures.[79] Two parameters are then necessary for defining the activation barriers for the forward and backward reactions: the solvent reorganization energy

$$\lambda_s=\lambda^{\mathrm{I}}+\lambda^{\mathrm{II}} \tag{17}$$

and the equilibrium free energy gap $\Delta F_0=(\langle\Delta E\rangle_1+\langle\Delta E\rangle_2)/2$. The present formulation is limited to the Marcus LRA scheme. Nonlinear effects, necessitating more than two parameters for defining the ET free energy surfaces,[80,81] are not considered here.

The LRA is commonly verified by checking the quadratic dependence of the solvation chemical potential on the solute charge for ionic solutes or on the solute dipole for dipolar solutes. In the latter case, the LRA implies that the ratio

$$\frac{\mu_p(m_0)}{m_0}=\frac{1}{m_0}\int_0^{m_0}\frac{u_p(x)}{x}dx \tag{18}$$

is a linear function of m_0. Here $\mu_p(m_0)$ is the solvation chemical potential and $u_p(m_{0i})=\langle V_i\rangle$ is the average solute–solvent interaction energy; m_{0i} is the solute dipole in the ith electronic state and m_0 is used for changing solute dipole. Figure 5 shows $\mu_p(m_0)/m_0$ versus $m_0^*=(\beta m_0^2/\sigma^3)^{1/2}$ for a dipolar solvent with $m^*=1.0$ (squares) and a quadrupolar solvent with $m=0$ and the reduced quadrupolar moment $(Q^*)^2=\beta Q^2/\sigma^5=0.5$ (circles). The simulations were performed at different magnitudes of the solute dipole m_0; the average energies $u_p(m_0)$ were fitted to a polynomial in $(m_0^*)^2$ and then used for integration over the solute dipole in Eq. (18) (solid lines in Fig. 5).

The range of m_0^* values for which the LRA should be tested is dictated by the problem under consideration. The reaction field R_p of the nuclear solvent polarization, acting on a dipolar DAC in the ET activated state, is defined by the

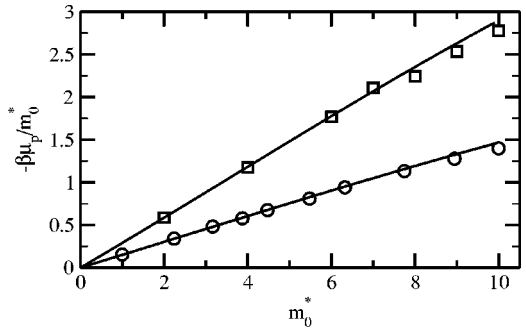

FIG. 5. $-\beta\mu_p/m_0^*$ vs m_0^* for solvation of a HS solute with the radius $R_0/\sigma=0.9$ in a dipolar solvent ($m^*=1.0$, squares) and in a quadrupolar solvent [$(Q^*)^2=0.5$, circles]. The dots are $-\beta u_p/2m_0^*$ and the solid lines are obtained by integration of a polynomial fit of $u_p(m_0^*)$ according to Eq. (18); $\rho^*=0.8$.

average vertical free energy gap $\langle\Delta E\rangle$ (energy of the charge-transfer optical transition) and the difference dipole in the final and initial states Δm_0,

$$R_p^{\ddagger}=\frac{\langle\Delta E\rangle}{\Delta m_0}. \tag{19}$$

Here we omit the subscript i to indicate that Eq. (19) can be applied to either the direct, $i=1$, or backward, $i=2$, transitions. The nonequilibrium reaction field of the activated ET state corresponds to equilibrium solvation of a fictitious dipole with magnitude

$$m_0=\frac{R_p^{\ddagger}}{2a_p}=\frac{\beta\langle\Delta E\rangle}{2\beta a_p\Delta m_0}, \tag{20}$$

where a_p is a response function of the nuclear solvent polarization such that the LRA chemical solvation potential of a dipole is $\mu_p=-a_p m_0^2$. With the slope of $\beta\mu_p/m_0^*$ versus m_0^* in Fig. 5 equal to $a_p\sigma^3=0.58$, m_0^* is equal to 10 in Eq. (20) when $\beta\langle\Delta E\rangle=20$. Testing the LRA for higher vertical energy gaps of the order of $\beta\langle\Delta E\rangle\simeq 80$ often encountered in spectroscopic applications requires simulations with higher m_0^*. We will assume that the LRA holds in all calculations below in the range of solvent polarities $(m^*)^2\leqslant 6$ for which the simulations of charged and neutral diatomics show $\lambda_1\simeq\lambda_2$ (Fig. 4).

The validity of the LRA opens an important route to the formulation of analytical theories of ET reorganization. Treatment of orientationally dependent, long-range multipolar interactions between the solute and solvent is a complex task for both analytical modeling and computer simulations. The fact that the reorganization energy is state independent allows us to calculate λ_s as the variance of the solute–solvent interaction potential taken on the solvent configurations in equilibrium with a nonpolar DAC (D–A diatomic in MC simulations) without charges on the donor and acceptor defining the ET dipole.[82] This approach will be utilized in Sec. IV below.

B. Orientational and density fluctuations

The solvent reorganization energy reflects the energetic intensity of nuclear fluctuations created by thermal excitations of collective modes of the solvent. Each such collective mode is characterized by its symmetry and the length of the correlation decay (correlation length Λ). Anisotropic fluctuations of dipolar polarization and isotropic fluctuations of density are two major collective modes in polar molecular liquids.[6,45] The wave vector $\mathbf{k}$ of the inverted space creates axial symmetry in the otherwise isotropic polar liquid. Accordingly, two projections are sufficient to define the nuclear polarization filed $\tilde{\mathbf{P}}_n'(\mathbf{k})$: the longitudinal polarization $\tilde{P}^L(\mathbf{k})=\hat{\mathbf{k}}\cdot\tilde{\mathbf{P}}_n'(\mathbf{k})$ and the transverse polarization $\tilde{P}^T(\mathbf{k})=|\tilde{\mathbf{P}}_n'(\mathbf{k})-\hat{\mathbf{k}}(\hat{\mathbf{k}}\cdot\tilde{\mathbf{P}}_n'(\mathbf{k}))|$ (the nuclear field $\mathbf{P}_n'$ is defined in Sec. III). The properties of thermal fluctuations of these two projections are substantially different because of the anisotropic nature of dipolar interactions.[11]

Fluctuations of the longitudinal polarization are short ranged (Fig. 2). The corresponding longitudinal correlation length Λ^L can be found from Wertheim's solution of the mean-spherical approximation (MSA) for dipolar HS molecules as[83]

$$\Lambda^L=3\sigma\xi/(1+4\xi), \tag{21}$$

where ξ is the MSA polarity parameter: $\xi\to 0$ when $\epsilon_s\to 0$ and $\xi\to 0.5$ when $\epsilon_s\to\infty$. Correspondingly, $\Lambda^L\to\sigma/2$ at $\epsilon_s\to\infty$. Correlation length Λ^L enters the effective solute radius of an ion in the MSA derivation of the Born equation for ion–dipolar mixtures,[84] $r_{\text{eff}}=R_0+\sigma/2-\Lambda^L$, where R_0 is the radius of a spherical ion.

In contrast to longitudinal polarization fluctuations with correlation length approaching its maximum value of $\sigma/2$ when $\epsilon_s\to\infty$, the transverse polarization fluctuations are macroscopic with the correlation length diverging when $\epsilon_s\to\infty$ (Fig. 2). In the MSA,[83]

$$\Lambda^T=3\xi\sigma/2(1-2\xi), \tag{22}$$

and one gets $\Lambda^T\to\infty$ at $\xi\to 0.5$. Here Λ^L and Λ^T define the asymptotic distance decay of the correlation function,

$$\langle\delta P^{L,T}(r)\,\delta P^{L,T}(0)\rangle\propto r^{-1}e^{-r/\Lambda^{L,T}}. \tag{23}$$

The longitudinal and transverse fluctuations of the dipolar polarization in a polar solvent are described by the longitudinal, $S^L(k)$, and transverse, $S^T(k)$, structure factors:

$$S^L(k)=\frac{3}{N}\sum_{i,j}\langle(\hat{\mathbf{e}}_i\cdot\hat{\mathbf{k}})(\hat{\mathbf{k}}\cdot\hat{\mathbf{e}}_j)e^{i\mathbf{k}\cdot\mathbf{r}_{ij}}\rangle, \tag{24}$$

$$S^T(k)=\frac{3}{2N}\sum_{i,j}\langle[(\hat{\mathbf{e}}_i\cdot\hat{\mathbf{e}}_j)-(\hat{\mathbf{e}}_i\cdot\hat{\mathbf{k}})(\hat{\mathbf{k}}\cdot\hat{\mathbf{e}}_j)]e^{i\mathbf{k}\cdot\mathbf{r}_{ij}}\rangle, \tag{25}$$

where $\mathbf{r}_{ij}=\mathbf{r}_i-\mathbf{r}_j$. Here, and throughout below, carets are used for unit vectors; e.g., $\hat{\mathbf{e}}_j$ is a unit vector in the direction of the solvent dipole. The structure factors can be connected to the correlators of $\delta\tilde{P}^L(k)$ and $\delta\tilde{P}^T(k)$,

$$S^L(k)=\frac{3}{N(m')^2}\langle|\delta\tilde{P}^L(k)|^2\rangle \tag{26}$$

and

$$S^T(k)=\frac{3}{2N(m')^2}\langle|\delta\tilde{P}^T(k)|^2\rangle. \tag{27}$$

In Eqs. (24)–(27), the average $(\cdots)$ is taken over the equilibrium configurations of the pure solvent of N molecules and m' is the liquid-state dipole moment of the solvent molecules (see Sec. III below).

The connection between the microscopically defined structure factors and macroscopic dielectric functions of a polarizable solvent involves some mean-field arguments.[11] The longitudinal and transverse macroscopic response functions can be defined in terms of correlators of the total polarization of the solvent:

$$\mathbf{P}_t=\mathbf{P}_n+\mathbf{P}_e, \tag{28}$$

where $\mathbf{P}_n$ and $\mathbf{P}_e$ are the nuclear and electronic polarization, respectively. The longitudinal and transverse correlators are then given by the relations

$$\begin{aligned}\chi_t^L&=\frac{1}{4\pi}(1-\epsilon_s^{-1})=\frac{\beta}{\Omega}\lim_{k\to 0}\langle|\delta\tilde{P}_t^L(k)|^2\rangle,\\ \chi_t^T&=\frac{1}{2\pi}(\epsilon_s-1)=\frac{\beta}{\Omega}\lim_{k\to 0}\langle|\delta\tilde{P}_t^T(k)|^2\rangle,\end{aligned} \tag{29}$$

where Ω is the solvent volume. The above average can be taken in the mean-field approximation for the solvent-induced dipoles:

$$\begin{aligned}\frac{\beta}{\Omega}\lim_{k\to 0}\langle|\delta\tilde{P}_t^L(k)|^2\rangle&=3\rho s^L\alpha+[\beta\rho m^2(s^L)^2/3]S^L(0),\\ \frac{\beta}{\Omega}\lim_{k\to 0}\langle|\delta\tilde{P}_t^T(k)|^2\rangle&=6\rho s^T\alpha+[2\beta\rho m^2(s^T)^2/3]S^T(0),\end{aligned} \tag{30}$$

where the factors s^L and s^T account for the renormalization of the vacuum solvent polarizability α and dipole moment m by the self-consistent field of the induced dipoles.[85] From the condition that $\epsilon_s=\epsilon_\infty$ at $m=0$ one gets $s^L=(\epsilon_\infty+2)/3\epsilon_\infty$ and $s^T=(\epsilon_\infty+2)/3$, which leads to the following relation between the $k=0$ values of two structure factors:

$$\frac{S^L(0)}{S^T(0)}=\frac{\epsilon_\infty}{\epsilon_s}. \tag{31}$$

Equation (31) was obtained previously by Madden and Kivelson from somewhat different arguments.[11] If one defines $y_p=(4\pi/9)\beta\rho(ms^L)^2$ (Ref. 20), the equations for the structure factors at $k=0$ become

$$\begin{aligned}S^L(0)&=c_0/3y_p,\\ S^T(0)&=(\epsilon-\epsilon_\infty)/3\epsilon_\infty^2 y_p.\end{aligned} \tag{32}$$

Note that Eq. (32) leads to the Fröhlich–Kirkwood expression[14] for the Kirkwood factor:

$$\begin{aligned}g_K&=\frac{1}{3}[S^L(0)+2S^T(0)]\\ &=\frac{(\epsilon_s-\epsilon_\infty)(2\epsilon_s+\epsilon_\infty)}{9y_p\epsilon_s\epsilon_\infty^2}=\frac{(\epsilon_s-\epsilon_\infty)(2\epsilon_s+\epsilon_\infty)}{y\epsilon_s(\epsilon_\infty+2)^2}.\end{aligned} \tag{33}$$

The different nature of the longitudinal (short-range) and transverse (long-range) polarization fluctuations is reflected in the behavior of $S^L(k)$ and $S^T(k)$ at small wave vectors $k<2\pi/\sigma$. Dipoles collinear to an external electric field (longitudinal polarization) tend to be antiparallel [Fig. 6(a)]. If one assumes a hexagonal alignment of dipoles in the first coordination sphere of a given dipole, then two tail-to-head dipoles are preferentially parallel to the central dipole whereas four side-to-side dipoles are antiparallel. This creates effectively two antiparallel dipoles in the first coordination sphere of each dipole in the solvent. Their correlation brings a negative sign to $i\neq j$ term in Eq. (24), leading to $S^L(0)<1$. This behavior is similar to that of another type of short-range correlations in dense liquids: the density fluctuations. In the latter case, the $k=0$ value of the density structure factor $S(0)$ is also less than 1 (Fig. 7), becoming greater than 1 close to the critical point when density fluctuations become long ranged.[86] Rotations of dipoles out from parallel alignment with an external field tend to add up in the transverse polarization due to Coulomb attraction of opposite charges[87] [Fig. 6(b)], resulting in $S^T(0)>1$ (Fig. 7) characteristic of long-range correlations.

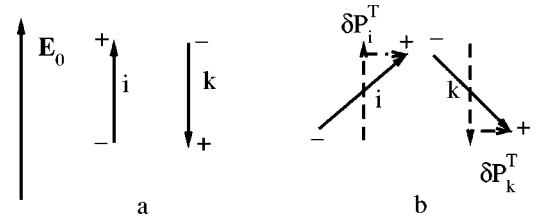

FIG. 6. Preferential antiparallel orientation of dipoles i and k collinear with the external field $\mathbf{E}_0$ (a). Transverse polarization created by librational fluctuations of orientations of dipoles i and k adds up because of the Coulomb attraction between negative and positive ends of the polar molecules (b).

Density fluctuations occur on the molecular scale of the order of the molecular diameter with the correlation length from the Percus–Yevick (PY) solution for a HS fluid as[88]

$$\Lambda^D=3\sigma\eta/2(1+2\eta). \tag{34}$$

Here η is the solvent packing density defined as fraction of the volume of the solvent molecules Ω_s in the total volume Ω occupied by the solvent, $\eta=\Omega_s/\Omega$ ($\eta\cong 0.4$–0.55 for molecular liquids at normal conditions). The correlation length Λ^D defines the long-distance decay of the density correlation function,

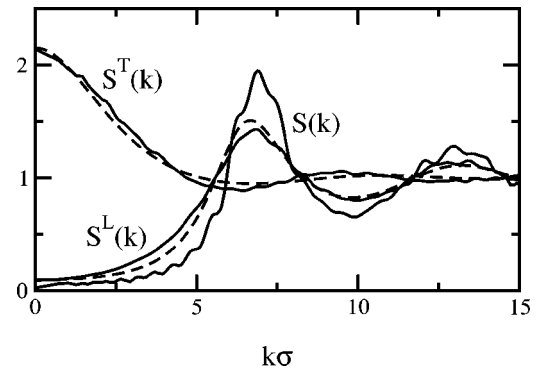

FIG. 7. Density $[S(k)]$, longitudinal $[S^L(k)]$, and transverse $[S^T(k)]$ structure factors for a liquid with $(m^*)^2=3.0$ and $(Q^*)^2=0.5$. The solid lines are the results of MC simulations and the dashed lines show the calculations with the PPSF; $\rho^*=0.8$.

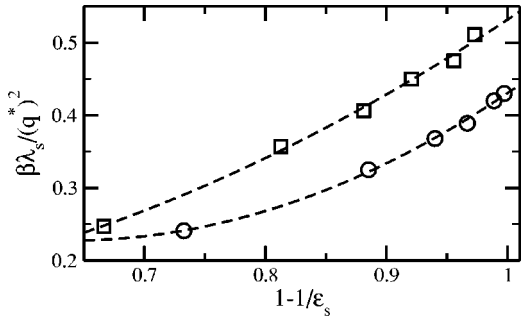

FIG. 8. λ_s from MC simulations of a neutral diatomic D–A vs $1-1/\epsilon_s$ obtained from separate simulations of corresponding pure solvents. Circles correspond to dipolar solvents (m is varied) and squares are for dipolar–quadrupolar solvents [$(Q^*)^2=0.5$ and m is varied].

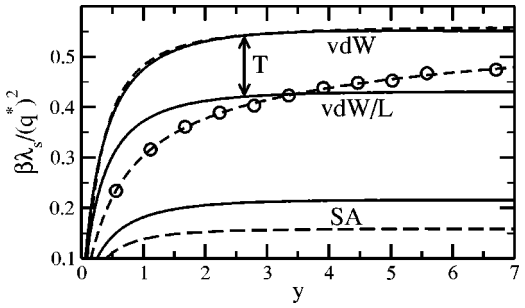

FIG. 9. λ_s from MC simulations of a charged diatomic (circles) and from continuum longitudinal response with the van der Waals cavity [Eq. (1), vdW/L]. The dashed line refers to the Marcus formula [Eq. (38)]; $R_A/\sigma=R_D/\sigma=0.9$ and $R/\sigma=1.8$. DELPHI calculations are shown for the solvent-accessible (SA) van der Waals (vdW) cavities. The vertical arrow connecting vdW/L and vdW solutions indicates the contribution of transverse polarization to continuum calculations. The reduced charge q^* is defined by Eq. (A2).

$$\langle \delta\rho(r)\,\delta\rho(0)\rangle \propto r^{-1}e^{-r/\Lambda^D}. \tag{35}$$

Both the long-distance and short-distance behavior of the density correlations are described by the density structure factor

$$S(k)=1+\rho\tilde{h}_{ss}^{000}(k) \tag{36}$$

in which $\tilde{h}_{ss}^{000}(k)$ stands for the spherically symmetric component of the solvent–solvent (subscript "ss") pair correlation function.[45]

C. Polarity dependence

The Marcus approximate relation for λ_s employs the longitudinal field of the ET dipole (transverse component is neglected) in the form

$$\Delta\tilde{E}_0^L(\mathbf{k})=\frac{4\pi ie}{k}[j_0(kR_D)-j_0(kR_A)e^{i\mathbf{k}\cdot\mathbf{R}}], \tag{37}$$

where R_D and R_A are the radii of the spherical donor and acceptor units, respectively, R is the D–A distance, and e is the elementary charge; $j_n(x)$ is the spherical Bessel function of order n. The substitution of Eq. (37) into Eqs. (1) and (2) leads to the relation

$$\lambda_s^{\mathrm{M}}=\frac{e^2c_0}{2}\left(\frac{1}{R_D}+\frac{1}{R_A}-\frac{2}{R}\right), \tag{38}$$

with λ_s^{M} proportional to the Pekar factor c_0 [Eq. (1)]. Although $\lambda_s\propto c_0$ is strictly valid only for spherically symmetric cavities, it holds surprisingly well.[89] This is illustrated in Fig. 8 where λ_s obtained from simulations of the D–A diatomic is plotted against $1-1/\epsilon_s(\epsilon_\infty=1)$ with ϵ_s obtained from simulations of pure dipolar and dipolar–quadrupolar solvents. There is a noticeable curvature of λ_s versus $1-1/\epsilon_s$ in purely dipolar solvents, which almost disappears when an axial solvent quadrupole is added. The addition of the quadrupole moment weakens the dependence of ϵ_s on $(m^*)^2$ (Table I), resulting in a nearly linear trend of λ_s versus $1-1/\epsilon_s$.

The existence of a linear trend of λ_s with the Pekar factor does not, however, mean that the Marcus formula (1) and/or (38) provide accurate values for λ_s. Dielectric continuum calculations are strongly affected by the definition used to specify the dielectric cavity. Various approaches encountered in the literature can generally be referred to the van der Waals (vdW) cavity and the solvent-accessible (SA) cavity. In the former definition, the dielectric cavity is the space excluded from the solvent by the vdW repulsive core of the solute. For the SA cavity, the discrete size of the solvent molecules is taken into account by adding the solvent radius to the vdW radii of atoms or molecular groups exposed to the solvent. Notice that the SA cavity is more consistent with microscopic solvation theories as they convert to dielectric models with the SA cavity in the $k\to 0$ limit for the microscopic response functions.

When only longitudinal polarization is taken into account in the calculation of λ_s with the SA cavity, the result is too small. Longitudinal λ_s [Eq. (1)] with the vdW cavity turns out to be reasonably close to simulations (marked vdW/L in Fig. 9). The calculations according to Eq. (1) were done by taking the numerical Fourier transform of $\Delta\mathbf{E}_0$ for the diatomic with radii $R_D=R_A$ and $R=R_D+R_A$. The longitudinal projection of $\Delta\tilde{\mathbf{E}}_0$ was then used in Eq. (2) to calculate the longitudinal electrostatic energy. The Marcus equation for the diatomic with vdW cavity [Eq. (38), upper dashed line in Fig. 9] overestimated λ_s by about 60% in the medium polarity range. This equation is not strictly applicable to the contact donor–acceptor configuration, but it does not provide an acceptable accuracy also when the donor–acceptor distance is significantly increased as is seen from the following section.

A full solution of the Poisson equation for the $\mathrm{D}^+-\mathrm{A}^-$ diatomic was obtained by employing the finite-difference DELPHI solver.[90] This package uses the vdW cavity with slight modifications incorporated in the definition of the "molecular surface."[91] With the dielectric cavity defined by two spheres of the donor and acceptor, the reduced reorganization energy $\beta\lambda_s/(q^*)^2$ obtained from DELPHI (labeled vdW in Fig. 9) is very close to the Marcus equation (dashed line in Fig. 9). The use of the SA cavity in the full Poisson solution (labeled SA in Fig. 9) leads to too low λ_s compared to simulations. The Marcus equation reproduces well the full solution of the Poisson equation for DA diatomics with $R>R_D+R_A$, but deviates, as expected, from the Poisson

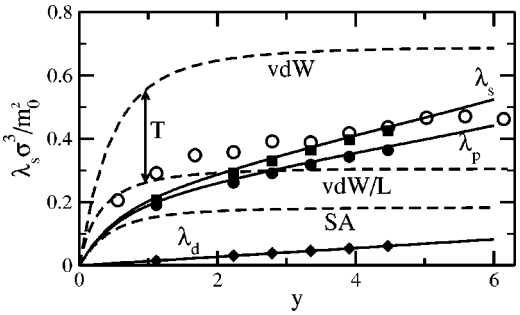

FIG. 10. λ_s vs y obtained from MC simulations (Ref. 81) (open circles) and the NRFT (lines and solid points) for a spherical dipolar solute. The dashed lines refer to the Onsager continuum solution [Eq. (39)] with the cavity radius equal to the solute radius R_0 (upper line, vdW) and the cavity radius equal to $R_1=R_0+\sigma/2$ (lower line, SA). The middle dashed line (vdW/L) indicates the longitudinal reorganization energy calculated with the vdW cavity [Eq. (40)]. The vertical arrow connecting vdW/L and vdW solutions indicates the contribution of transverse polarization to continuum calculations. The solid lines refer to λ_s calculated within the NRFT from Eqs. (67) and (99) with the use of the PPST/PY for the structure factors. Solid points refer to the same calculations with the structure factors obtained from MC simulations.

equation solution for $R<R_D+R_A$ (lower curves labeled SA in Fig. 9). The vertical arrow in Fig. 9 indicates the gap between the full solution of the Poisson equation and the longitudinal reorganization energy. This gap, amounting about 25% for this donor–acceptor configuration, is the contribution of the transverse polarization to the continuum λ_s.

Similarly to the diatomic solute, the simulated reorganization energies[81] for a dipolar spherical solute (circles in Fig. 10) fall in between of two continuum results for the vdW and SA cavities (dashed lines in Fig. 10). The solution of the Poisson equation is known analytically in this case and is given by the Onsager reaction-field expression.[71] For the SA cavity it becomes

$$\lambda_s=\frac{m_0^2}{R_1^3}\frac{\epsilon_s-1}{2\epsilon_s+1}, \tag{39}$$

where $R_1=R_0+\sigma/2$. Similarly to the case of the diatomic solute, the use of combination of Eq. (1) with the vdW cavity gives a reasonable estimate for λ_s which becomes in this case ($\epsilon_\infty=1$)

$$\lambda_s=\frac{2m_0^2c_0}{9R_0^3}. \tag{40}$$

Calculations for both types of solutes considered here show a very high sensitivity of the dielectric models to the choice of the dielectric cavity, rendering all such calculations strongly dependent on the assumptions made to represent a molecular system by a continuous medium.

In addition to quantitative uncertainties with continuum reorganization energies, there are also qualitative problems. The initial rise of λ_s with increasing solvent dipole is not as sharp as the Pekar factor would predict. More importantly, dielectric continuum models give saturation of λ_s starting from moderately polar solvents with $y\geqslant 2$. This is not reproduced by simulations. Instead of reaching a saturation limit, the reorganization energy continues to grow approximately linearly with y. A qualitatively similar result has been previously obtained for solvation of a point dipole.[81] A saturation limit of the solute–solvent average interaction energy was reached in those simulations only when the LRA broke down due to nonlinear dewetting of the solute surface in highly polar solvents.

On a more fundamental level, the clear difference between reorganization energies obtained from the longitudinal polarization only [Eq. (1)] and from the full Poisson equation puts under question the Marcus concept of longitudinal polarization fluctuations as the main collective solvent mode driving ET. The solution of the Poisson equation, including both longitudinal and transverse polarization modes, supports the notion that each component of polarization participates in ET energetics. The dynamics of these two modes are, however, distinctly different: the relaxation time of longitudinal fluctuations, τ^L, is considerably shorter in polar solvents than the relaxation time of transverse fluctuations τ^T (Ref. 92). The extended hydrodynamic description of polarization dynamics by Bagchi and Chandra[6] leads to microscopic relaxation times for longitudinal and transverse polarization fluctuations which both depend on k,

$$\tau^{L,T}(k)=D(k)^{-1}S^{L,T}(k), \tag{41}$$

where $D(k)=2D_R+k^2D_T$, and D_R and D_T are the rotational and translational diffusion coefficients, respectively. In the long-wavelength limit $k\to 0$, one obtains, from Eqs. (31) and (41), $\tau^L(0)/\tau^T(0)=\epsilon_\infty/\epsilon_s$.

If transverse and longitudinal polarization modes participate comparably in ET activation, the effect of solvent dynamics on ET should reveal two significantly different characteristic relaxation times.[93] This is not observed in experiment which for the most part indicates that τ^L, or shorter time scales,[94] is the characteristic time relevant to ET dynamics.[7] Solvation dynamics[10] also point to τ^L as the characteristic time responsible for the long-time portion of the dynamic response function. Therefore, continuum electrostatics calculations seem to come in contradiction with time-resolved experiments. An additional support to the longitudinal activation mechanism is provided by the experimentally observed proportionality between λ_s and c_0 (Ref. 89) and a similar approximately linear trend of λ_s versus c_0 from the present simulations shown in Fig. 8. The analytical theory developed in Sec. IV resolves the puzzle. It turns out that the microscopic formulation of the theory leads to a predominantly longitudinal polarization response thus confirming the qualitative picture of the Marcus model.

D. Distance dependence

The reorganization energy λ_s is predicted to vary with the donor–acceptor distance according to the Coulomb law in Eq. (38). This prediction has been tested here on MC simulations of equal-size donor and acceptor spheres at various separations in a dipolar solvent with $(m^*)^2=3.0$ and the results are shown in Fig. 11. As above, the simulations were performed for two charge configurations of the DAC: circles in Fig. 11 indicate uncharged spheres (D–A diatomic) whereas diamonds refer to the DAC with two opposite charges (D^+-A^- diatomic). As is seen, the LRA holds ex-

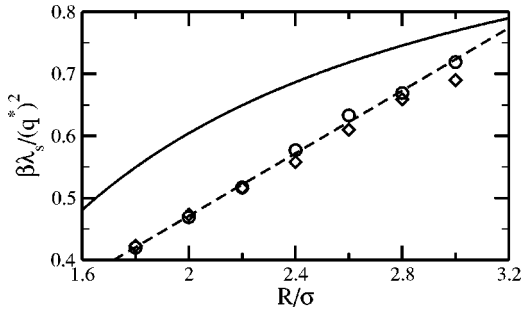

FIG. 11. λ_s vs the distance between spherical donor and acceptor from MC simulations (points) and from Eq. (38) (solid line). Circles correspond to uncharged DAC, and diamonds refer to the D^+-A^- DAC; $(m^*)^2=3.0$, $(Q^*)^2=0$, $\rho=0.8$, and $R_{D,A}/\sigma=0.9$. The dashed line is a regression drawn through the circles.

ceptionally well for all simulated configurations. Further, λ_s changes linearly with R in the simulated range of distances going from the contact to solvent-separated configuration of the DAC. This dependence is slightly different from the curved-up Coulomb law and can be explained by the effects of changing the solvation shell of the donor and acceptor with increasing separation. Finally, there is no discontinuity in λ_s when the solvent-separated configuration is created and a dipolar solvent molecule gets trapped between the opposite charges on the donor and acceptor ($R/\sigma \geqslant 2.8$ in Fig. 11). This result is an indication of the many-body character of the polarization response making λ_s insensitive to local structural modifications involving only one solvent molecule.

E. Range of the solvent–solvent interaction and the continuum limit

As defined by Eq. (9), the solvent reorganization energy is proportional to β, $\lambda_s \propto \beta$. This strong dependence on temperature disagrees with no explicit temperature dependence of the reorganization energy obtained from the fluctuation–dissipation theorem[95,96] and from dielectric cavity models.[15,18] The cancellation of the β factor occurs for the charge–dipole solute–solvent coupling because of the long-range character of dipolar correlations in polar solvents.

In the limit of large donor and acceptor units in the DAC, $2R_{D,A}/\sigma \gg 1$ (R_D and R_A are the effective radii of the donor and acceptor sites, respectively) the single-molecule and two-molecule terms in Eq. (11) can be combined together to give λ_s in the form

$$\lambda_s=(\beta/2)\Delta\tilde{v}*\tilde{F}_{ss}*\Delta\tilde{v}. \tag{42}$$

Here, and throughout below, we denote integration over the coordinates common to two functions by an asterisk and use ''tilde'' for the Fourier transform of the corresponding direct-space functions. A detailed account of the notation scheme used here is given in Appendix B.

The pair distribution function of the solvent

$$\tilde{F}_{ss}(12)=\rho\delta(12)+\rho^2\tilde{h}_{ss}(12) \tag{43}$$

can be expanded in a series of chain diagrams appearing in the γ expansion[45] and in the optimized cluster expansion of Andersen and Chandler:[97]

$$\tilde{F}_{ss}(12)=\sum_n C^{(n)}(12). \tag{44}$$

Here 1 and 2 stand for the coordinates and Euler angles of solvent molecules 1 and 2, respectively. In the above series, each summand $C^{(n)}(12)$ separates the long-range dipolar forces, represented by single $\tilde{\phi}$ bonds [$\tilde{\phi}=-\beta\tilde{v}_{ss}(k)$, where $\tilde{v}_{ss}(k)$ is the Fourier transform of the solvent–solvent multipolar interaction potential], from short-range correlations represented by composite ''self-energy'' graphs $\Sigma(1,2)=\rho\delta(12)+W(12)$.[98] For example, for $C^{(3)}(12)$, one has

$C^{(3)}(12)=$ 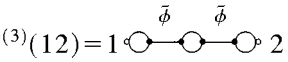 2

Here the solid line represents $\tilde{\phi}$, a large circle stands for the self-energy, and angular average is performed over the black circles each bringing in a ρ factor.

The long-range nature of dipole–dipole forces is reflected in the fact that $\tilde{\phi}$ does not vanish in the macroscopic limit $k\to 0$: $|\tilde{\phi}(0)|>0$.[99] This implied that an infinite series of chain diagrams as given by Eq. (44) should be included in the calculation of $\tilde{F}_{ss}(12)$ at $k=0$.[83] The $k\to 0$ limit of such calculations leads to

$$\lambda_s=\frac{3y_p}{8\pi}\sum_{p=L,T} S^p(0)\Delta\tilde{E}_0^p*(\Delta\tilde{E}_0^p)^*, \tag{45}$$

where now the β factor is accommodated into y_p [see Eq. (59) below for its definition] and $\Delta\tilde{E}_0^L$ and $\Delta\tilde{E}_0^T$ are, respectively, the longitudinal and transverse projections of the Fourier transform $\Delta\tilde{\mathbf{E}}_0$ [Eq. (3)]. The structure factors at $k=0$ are proportional to $1/y_p$ (Ref. 98) [Eq. (32)] and the y_p factor cancels from λ_s. There is therefore no explicit dependence on T, as expected from the macroscopic fluctuation–dissipation theorem. The disappearance of the β factor from λ_s is a result of a mutual cancellation of single-molecule and two-molecule components of the reorganization energy due to the long-range character of dipole-dipole interactions in the solvent.

The cancellation of the β factor does not happen for short-range solvent–solvent potentials $\propto 1/r^\delta$ with $\delta>3$. The Fourier transform $\tilde{v}_{ss}(k)$ then vanishes at $k\to 0$ (e.g., the dipole–quadrupole interaction potential $\tilde{v}_{ss}\propto k$ at $k\to 0$) and, in the macroscopic limit, one has

$$\lambda_s=(\beta/2)\Delta\tilde{v}(1)*\Sigma(12)*\Delta\tilde{v}(2). \tag{46}$$

Equation (46) can be considered as a molecular basis for the use of the continuum approximation to describe the reorganization energy arising from thermal fluctuations of short-range interaction potentials (quadrupolar solvation is an obvious target). The short-range correlation term $\Sigma(12)$ does not provide cancellation of the β factor and λ_s is proportional to β. This explicit dependence on temperature is responsible for a positive contribution to the reorganization entropy which often dominates in the total reorganization entropy.[20,38]

III. ELECTRONIC ENERGY LEVELS IN POLAR-POLARIZABLE SOLVENTS

The application of the LRA to the calculation of λ_s involves two steps: (i) the definition of the solute–solvent intermolecular potential and (ii) the calculation of the relevant solvent response functions. This section deals with the solute–solvent potential followed by the definition of the response function in the next section. The form of the response function appearing in the solvent reorganization energy is dictated by the symmetry of the solute–solvent potential and by the molecular shape of the solute. The dipole–charge approximation for the solute–solvent interaction potential [Eq. (14)] is based on the assumption that the distance l_{0s} between a solute charge and the center-of-charge distribution on a solvent molecule

$$\mathbf{r}_c=\left(\sum_k |q_k|\right)^{-1}\sum_k |q_k|\mathbf{r}_k \tag{47}$$

(q_k are partial charges with coordinates $\mathbf{r}_k$) is considerably larger than the distance between partial charges of the solvent molecule, $l_{ss}=\max|\mathbf{r}_k-\mathbf{r}_j|$. The definition of the charge–dipole potential is thus based on the first-order expansion in the smallness parameter:

$$\zeta_1=l_{ss}/l_{0s}\ll 1. \tag{48}$$

This condition usually holds for molecular DACs and is a reason why the dipolar approximation and, on a more coarse-grained level, the continuum models have served so well in treating the solvent effect on ET and optical spectra.[100] The symmetry of the dipole–charge solute–solvent interaction projects out two polarization structure factors $S^L(k)$ and $S^T(k)$ from the manifold of symmetries characterizing thermal fluctuations in a molecular solvent (see Sec. V below). These two structure factors enter the two-molecule component of λ_s [Eq. (13)]. The one-molecule response [Eq. (12)] is modulated by the local density fluctuations and hence includes the density structure factor $S(k)$. The latter can be taken from experiment,[88] while liquid-state theories or computer simulations are needed for the polarization structure factors.[59,101–105]

Up to this point, we have been considering nonpolarizable solvents. The MC simulations used to illustrate the qualitative properties of λ_s in Sec. II were also performed on nonpolarizable solvents. In order to describe λ_s in real solvents one needs to specify the solute–solvent interaction potential for the case of a DAC in a polar-polarizable dipolar solvent, each molecule of which bears an induced and a permanent dipole. The magnitude of the induced dipole is characterized by the dipolar polarizability α. In the present consideration, the DAC is assumed to be nonpolarizable. Solute polarizability effects have been included for spherical dipolar solutes.[65,106] A distributed polarizability density[107] is necessary for solutes of arbitrary geometry.

The transferred electron interacts by Coulomb forces with both electronic and nuclear charges of the solvent molecules. The ET system is characterized by at least three principal energy scales: the energy of electronic excitations of the solvent molecules, $\hbar\omega_e$, the ET transition energy $\hbar\omega_0=\Delta E^{\mathrm{ad}}$ (ΔE^{ad} is the adiabatic vacuum energy gap between the two ET states), and the characteristic energy of nuclear motions, $\hbar\omega_n$. When both ω_e and ω_0 are quantum ($\omega_e,\omega_0\gg k_BT$) and ω_e, $\omega_0\gg\omega_n$, one can eliminate the electronic degrees of the system by defining the instantaneous energies E_i (actually partial free energies) for each electronic state.[108] The energies E_i are obtained as the statistical average of the system density matrix over the electronic degrees of freedom ($\mathrm{Tr}_{\mathrm{el}}$):

$$e^{-\beta E_i}=\mathrm{Tr}_{\mathrm{el}}(e^{-\beta H_i}), \tag{49}$$

where H_i is the system Hamiltonian in the ith state ($i=1,2$). The energies E_i then define the fluctuating energy gap $\Delta E=E_2-E_1$ between the acceptor and donor electronic states, the variance of which gives the solvent reorganization energy [Eq. (9)].

The diabatic (no electronic overlap) Hamiltonian H_i of a localized electronic state in a polar medium characterized by induced and nuclear dipolar polarization can be written as

$$H_i=I_i+U^{\mathrm{rep}}+H[\mathbf{P}_e]-\mathbf{E}_{0i}*\mathbf{P}_t-\tfrac{1}{2}\mathbf{P}_t*\mathbf{T}*\mathbf{P}_t. \tag{50}$$

Here I_i are the eigenvalues of the gas-phase Hamiltonian for the initial ($i=1$) and final ($i=2$) electronic states. $\Delta I=I_2-I_1$ is the vertical energy gap implying that the crude adiabatic approximation[109] is used in respect to intramolecular skeletal vibrations.[30] In Eq. (50), U^{rep} stands for repulsion solute–solvent and solvent–solvent potentials. The total dipolar polarization defined by Eq. (28) is a sum of the nuclear

$$\mathbf{P}_n(\mathbf{r})=\sum_j \mathbf{m}_j\delta(\mathbf{r}-\mathbf{r}_j) \tag{51}$$

and electronic

$$\mathbf{P}_e(\mathbf{r})=\sum_j \mathbf{p}_j\delta(\mathbf{r}-\mathbf{r}_j) \tag{52}$$

components. In Eqs. (51) and (52), the sum runs over the solvent molecules; $\mathbf{m}_j$ and $\mathbf{p}_j$ denote permanent and induced dipoles, respectively. Finally, in Eq. (50), $\mathbf{T}(\mathbf{r}-\mathbf{r}')=\nabla_{\mathbf{r}}\nabla_{\mathbf{r}'}|\mathbf{r}-\mathbf{r}'|^{-1}$ is the second-rank tensor of the dipole–dipole interaction which is imposed to be zero inside the molecular cores of the solvent molecules.[110] When the electronic polarization $\mathbf{P}_e$ is a Gaussian stochastic field, the formulation can be conveniently recast in the form of the Drude model of fluctuating induced dipoles defined by the Hamiltonian $H[\mathbf{P}_e]$.[111–113]

From Eq. (50), the energies E_i are obtained by taking the trace over $\mathbf{P}_e$ according to Eq. (49). This yields[108]

$$E_i=E_i^{\mathrm{np}}+V_i-\tfrac{1}{2}\mathbf{P}_n*\mathbf{T}*\mathbf{P}_n', \tag{53}$$

where the energy of the nonpolar subsystem is $E_i^{\mathrm{np}}=I_i-\frac{1}{2}\mathbf{E}_{0i}\cdot\boldsymbol{\alpha}'\cdot\mathbf{E}_{0i}$ and the interaction potential with the nuclear solvent polarization reads

$$V_i=-\mathbf{E}_{0i}*\mathbf{P}_n', \tag{54}$$

Tracing the system density matrix over the electronic polarization of the solvent creates a nonlocal solvent polarizability[45,114]

$$\boldsymbol{\alpha}'=\alpha(\mathbf{1}-\alpha\mathbf{T})^{-1}. \tag{55}$$

In addition, the nuclear polarization is renormalized to[114]

$$\mathbf{P}_n' = (\mathbf{1} - \alpha \mathbf{T})^{-1} \cdot \mathbf{P}_n . \tag{56}$$

This renormalization accounts for the well-known enhancement of the solvent permanent dipoles by the electric field of the induced solvent dipoles.[45] Note that neither $\mathbf{P}_n$ nor $\mathbf{P}_n'$ is assumed to be a continuous polarization density used in continuum dielectric models. From the definition in Eq. (51), E_i can be rewritten as

$$E_i = E_i^{\mathrm{np}} + U^{\mathrm{rep}} - \sum_j \mathbf{E}_{0i} \cdot \mathbf{m}_j' - \tfrac{1}{2} \sum_{j \neq k} \mathbf{m}_j \cdot \mathbf{T}_{jk} \cdot \mathbf{m}_k' , \tag{57}$$

where $\mathbf{T}_{jk} = \mathbf{T}(\mathbf{r}_j - \mathbf{r}_k)$ and

$$\mathbf{m}_j' = \sum_k \left(\mathbf{1} - \alpha \mathbf{T}\right)_{jk}^{-1} \cdot \mathbf{m}_k \tag{58}$$

is the effective condensed-phase solvent dipole. The corresponding microscopic dimensionless density of permanent dipoles is

$$y_p = (4\pi/9)\beta\rho(m')^2. \tag{59}$$

Equation (55) shows that, after tracing the induced solvent dipoles, the pure solvent is described by the Hamiltonian of a dipolar nonpolarizable solvent with the effective permanent dipoles $(mm')^{1/2}$. An external field, however, interacts with m' and this is the reason why m' and not $(mm')^{1/2}$ appears in the equations related to dielectric properties of the solvent obtained as linear response to an external electric field.[45]

IV. SOLVENT REORGANIZATION ENERGY

The formalism of nonlocal response functions developed here aims at expressing λ_s in terms of the molecular shape of the solute and parameters characteristic of the pure solvent. The solvent thermal motions are projected onto two solvent structure factors: the density structure factor and the dipolar polarization structure factor. The latter is split into its longitudinal and transverse components, reflecting the anisotropy of the dipole–dipole interactions.

The free energy surfaces of ET, $F_i(X)$, can be represented by a Fourier integral of the generating functional $\mathcal{G}_i(\zeta)$:

$$e^{-\beta F_i(X)} = \int_{-\infty}^{\infty} \frac{d\zeta}{2\pi} e^{i\zeta(X - \Delta E^{\mathrm{np}})} \mathcal{G}_i(\zeta), \tag{60}$$

where X is the energy gap reaction coordinate, $\Delta E^{\mathrm{np}} = E_2^{\mathrm{np}} - E_1^{\mathrm{np}}$, and

$$\mathcal{G}_i(\zeta) = Q_B^{-1} \mathrm{Tr}\left[e^{(i\zeta \Delta \mathbf{E}_0 + \beta \mathbf{E}_{0i}) * \mathbf{P}_n' - \beta U^{\mathrm{rep}} - \beta H_B} \right]. \tag{61}$$

Here $Q_B = \mathrm{Tr}(\exp[-\beta H_B])$ and H_B describes the nuclear subsystem of the pure solvent (thermal bath).

The generating functional can be expanded in Mayer functions defined on the solute–solvent interaction potential.[20,32] The exact result of this expansion is

$$\begin{aligned} \ln \mathcal{G}_i(\zeta) = \rho \int f_i(1,\zeta) d\Gamma_1 \\ + (\rho^2/2) \int f_i(1,\zeta) f_i(2,\zeta) h_{ss}(12) d\Gamma_1 d\Gamma_2 + (\rho^3/6) \\ \times \int f_i(1,\zeta) f_i(2,\zeta) f_i(3,\zeta) h_{ss}(123) d\Gamma_1 d\Gamma_2 d\Gamma_3 \\ + \cdots, \end{aligned} \tag{62}$$

with

$$f_i(1,\zeta) = e^{\mathbf{m}_1' \cdot [i\zeta \Delta \mathbf{E}(\mathbf{r}_1) + \beta \mathbf{E}_{0i}) - \beta U^{\mathrm{rep}}(\mathbf{r}_1)} - 1 \tag{63}$$

and $h_{ss}(12)$ and $h_{ss}(123)$ standing for, respectively, the pair and three-particle correlation functions of the pure solvent.

The Gaussian (LRA) approximation follows from Eq. (62) by expanding the Mayer functions in powers of ζ and truncating the expansion after the second order. The result of this procedure is the solvent reorganization energy given as a sum of two components:[20,32]

$$\lambda_s = \lambda_p + \lambda_d . \tag{64}$$

The first component reflects the energetic strength of anisotropic fluctuations of the solvent polarization (orientational reorganization energy[20]):

$$\lambda_p = \tfrac{1}{2} \Delta \tilde{\mathbf{E}}_0 * \boldsymbol{\chi} * \Delta \tilde{\mathbf{E}}_0^* , \tag{65}$$

where the asterisk in $\Delta \tilde{\mathbf{E}}_0^*$ stands for complex conjugate. The polarization response function is defined on the polarization structure factors

$$\begin{aligned} \boldsymbol{\chi}(\mathbf{k}_1 - \mathbf{k}_2) &= \delta_{\mathbf{k}_1, \mathbf{k}_2} \boldsymbol{\chi}_s(\mathbf{k}_2), \\ \boldsymbol{\chi}_s(\mathbf{k}) &= \frac{3y_p}{4\pi} [S^L(k)\mathbf{J}^L + S^T(k)\mathbf{J}^T], \end{aligned} \tag{66}$$

where $\mathbf{J}^L = \hat{\mathbf{k}}\hat{\mathbf{k}}$, $\mathbf{J}^T = \mathbf{1} - \hat{\mathbf{k}}\hat{\mathbf{k}}$, y_p is given by Eq. (59), and $\delta_{\mathbf{k}_1, \mathbf{k}_2} = (2\pi)^3 \delta(\mathbf{k}_1 - \mathbf{k}_2)$. The orientational reorganization energy in Eq. (65) is given in terms of the response of the pure solvent restricted to the volume outside the DAC.

The component λ_d in Eq. (64) describes the alteration of the solvent response by the local density profile of the solvent around the solute. It is built on the density structure factor and is called the density reorganization energy.[20,32] If three-molecule and all higher-order correlation functions are dropped from Eq. (62), the component λ_d becomes[32]

$$\lambda_d = -\frac{3y_p}{8\pi} \Delta \tilde{\mathbf{E}}_0 * (S - 1)\, \theta_0 * \Delta \tilde{\mathbf{E}}_0^* , \tag{67}$$

where the kernel $\theta_0(\mathbf{k}_1 - \mathbf{k}_2)$ projects the response inside the solute volume Ω_0:

$$\theta_0(\mathbf{k}_1 - \mathbf{k}_2) = \int_{\Omega_0} e^{i(\mathbf{k}_1 - \mathbf{k}_2) \cdot \mathbf{r}} d\mathbf{r}. \tag{68}$$

Note that Ω_0 is the space inaccessible to the solvent—i.e., a region surrounded by the SA surface (Sec. II C).

There is a mathematical and physical similarity between the reorganization components arising from orientational and density correlations. In order to make it clear we rewrite Eqs. (64)–(67) as

$$\lambda_s = 3y_p\mathcal{E}_0 + \frac{3y_p}{8\pi}\sum_{p=L,T}\Delta\tilde{E}_0^p*(S^p-1)*(\Delta\tilde{E}_0^p)* - \frac{3y_p}{8\pi}\Delta\tilde{\mathbf{E}}_0*(S-1)\,\theta_0*\Delta\tilde{\mathbf{E}}_0^*. \quad (69)$$

The first term in Eq. (69) is the electrostatic energy of the ET dipole in a uniform medium outside the solute characterized by the dipolar density y_p:

$$\mathcal{E}_0 = (8\pi)^{-1}\int_\Omega \Delta\mathbf{E}_0(\mathbf{r})^2 d\mathbf{r} = (8\pi)^{-1}\sum_{p=L,T}\Delta\tilde{E}_0^p*(\Delta\tilde{E}_0^p)*. \quad (70)$$

This term arises from the one-particle response λ^{I} representing changes in orientations and positions of a single solvent molecule not hindered by the restoring field of its neighbors. In a dense liquid solvent, molecular motions are affected by the restoring electric field of the surrounding molecules and by their repulsive cores. These two effects are represented by the second and third summands in Eq. (69), respectively. As discussed in Sec. II A, strong orientational correlations among the solvent dipoles cancel almost completely the electrostatic energy term $3y_p\mathcal{E}_0$. The density correlations are more short ranged and give a smaller contribution to λ_s. They are, however, significant for the reorganization entropy due to an explicit $1/T$ temperature dependence (Sec. II E).[20,32] The density reorganization term disappears in the limit of a macroscopic solute when only the orientational component is significant, $\lambda_s=\lambda_p$, and the reorganization energy tends to its continuum limit given by Eq. (45) (see Sec. VI C for the criterion of applicability of continuum models).

Equations (45) and (69) highlight problems arising with simple perturbation (and Mayer function) formulations for λ_p. If the difference field has only a longitudinal component, as in the Marcus formulation in Eqs. (1) and (37), Eq. (45) transforms into Eq. (1). When $\Delta\tilde{E}_0^T$ is nonzero, the continuum estimate of the transverse reorganization term [Eq. (45)]

$$\lambda_s^T = (\epsilon_s-1)\mathcal{E}_0^T \quad (71)$$

rises linearly with the solvent dielectric constant. The transverse electrostatic energy

$$\mathcal{E}_0^T = (8\pi)^{-1}\int\frac{d\mathbf{k}}{(2\pi)^3}|\Delta\tilde{E}_0^T|^2 \quad (72)$$

is often small compared to $\mathcal{E}_0^L$ for common ET systems. However, the factor (ϵ_s-1) in Eq. (71) makes λ_s^T grow strongly with increasing solvent polarity. This is not seen in MC simulations. Although simulations do not show saturation of λ_s predicted by the dielectric continuum models (Fig. 9), the growth of λ_s with solvent polarity is obviously slower than would appear from λ_s^T in Eq. (71). At large ϵ_s the term λ^T results in the "transverse catastrophe" of λ_s diverging with increasing ϵ_s. The flaw of Eq. (65) is that it does not incorporate the alteration of the polarization response by the insertion of the solute. The perturbation created by excluding polarization from the solute's volume propagates over a macroscopic distance due to the long-range length scale of transverse polarization fluctuations. This effect alters the continuum response function as is commonly accommodated into dielectric theories through cavity boundary conditions. Chandler's Gaussian model was designed to include this alteration of the response function on the microscopic length scale.[54–56] Below, we adopt this approach to reformulate the expression for λ_p.

In the Gaussian model, the generating functional is obtained through functional integration over the nuclear polarization field:[55,56]

$$\mathcal{G}(\zeta) = (Q_B)^{-1}\int e^{i\zeta\Delta\mathbf{E}_0*\mathbf{P}_n'-\beta H_B}\prod_{\Omega_0}\delta[\mathbf{P}_n'(\mathbf{r})]\mathcal{D}\mathbf{P}_n'. \quad (73)$$

Since the LRA holds for ET reorganization, it is sufficient to calculate the response function at $E_{0i}=0$ and, therefore, the interaction of the solute with the solvent is dropped from the statistical average [cf. Eqs. (61) and (73)]. In Eq. (73), the product Π_{Ω_0} is over the space points inside the solute thus excluding the solvent polarization from the solute volume.[115] The bath Hamiltonian H_B describes Gaussian fluctuations of the polarization field weighted with the polarization correlation function:

$$H_B = \tfrac{1}{2}\tilde{\mathbf{P}}_n'*\boldsymbol{\chi}^{-1}*(\tilde{\mathbf{P}}_n')*. \quad (74)$$

The functional integration in Eq. (73) leads to the orientational reorganization energy still defined by Eq. (65) with the polarization response function changed from $\boldsymbol{\chi}$ to a modified response function $\boldsymbol{\chi}^m$ given by the equation[54]

$$\boldsymbol{\chi}^m = \boldsymbol{\chi} - \boldsymbol{\chi}*\theta_0*\mathbf{G}^{-1}*\theta_0*\boldsymbol{\chi}. \quad (75)$$

Here the kernel $\mathbf{G}^{-1}(\mathbf{k}_1,\mathbf{k}_2)$ is the inverse of

$$\mathbf{G}(\mathbf{k}_1,\mathbf{k}_2) = \theta_0(\mathbf{k}_1-\mathbf{k}')*\boldsymbol{\chi}(\mathbf{k}'-\mathbf{k}'')*\theta_0(\mathbf{k}''-\mathbf{k}_2). \quad (76)$$

The kernel $\mathbf{G}$ can be rewritten in the form

$$\mathbf{G}(\mathbf{k}_1,\mathbf{k}_2) = \theta_0(\mathbf{k}_1-\mathbf{k}_2)[\boldsymbol{\chi}_s(\mathbf{k}_2)-\boldsymbol{\chi}'(\mathbf{k}_2)], \quad (77)$$

where

$$\boldsymbol{\chi}'(\mathbf{k}_2) = \int_{\Omega'}d\mathbf{r}\int e^{i(\mathbf{k}-\mathbf{k}_2)\cdot\mathbf{r}}\boldsymbol{\chi}_s(\mathbf{k})\frac{d\mathbf{k}}{(2\pi)^3}. \quad (78)$$

Here the region Ω' is outside the region Ω_0' made by the space points $\mathbf{r}_1-\mathbf{r}_2$ with $\mathbf{r}_{1,2}$ belonging to Ω_0.

Equation (75) is changed from the original formulation of the Gaussian model[54–56] in which the function $\boldsymbol{\chi}^m$ acts on the solute field not modified by the cutoff volume Ω_0. Instead, when Eq. (75) is used in Eq. (65) the response function acts on the solute field defined outside the DAC [Eq. (3)]. This transformation is achieved in terms of projections

of the response "in" and "out" of the DAC. The projection inside the DAC is defined by θ_0 in Eq. (68) while the projection outside the DAC is given by

$$\theta(\mathbf{k}_1-\mathbf{k}_2)=\int_\Omega e^{(\mathbf{k}_1-\mathbf{k}_2)\cdot\mathbf{r}}d\mathbf{r}. \tag{79}$$

The kernels θ_0 and θ satisfy the usual algebra of projection operators:

$$\begin{aligned}&\theta_0+\theta=\mathbf{1},\\&\theta_0*\theta=0,\\&\theta_0*\theta_0=\theta_0,\\&\theta*\theta=\theta,\end{aligned} \tag{80}$$

where $\mathbf{1}$ in Eq. (80) stands for $\delta_{\mathbf{k}_1,\mathbf{k}_2}$.

The substitution of Eqs. (77) and (78) into Eq. (75) leads to the response function

$$\boldsymbol{\chi}^m(\mathbf{k}_1,\mathbf{k}_2)=\boldsymbol{\chi}_s(\mathbf{k}_1)\delta_{\mathbf{k}_1,\mathbf{k}_2}-\boldsymbol{\chi}''(\mathbf{k}_1)\theta_0(\mathbf{k}_1-\mathbf{k}_2)\boldsymbol{\chi}_s(\mathbf{k}_2), \tag{81}$$

where $\boldsymbol{\chi}''=\boldsymbol{\chi}\cdot[\boldsymbol{\chi}-\boldsymbol{\chi}']^{-1}$ can be expressed through the longitudinal and transverse components of $\boldsymbol{\chi}'$ as

$$\boldsymbol{\chi}''=\mathbf{J}^L\frac{S^L}{S^L-\chi'^L}+\mathbf{J}^T\frac{S^T}{S^T-\chi'^T}. \tag{82}$$

Equations (81) and (82) give an exact solution for the renormalization of orientational polarization response in the presence of a solute of arbitrary form. From Eq. (81) the reorganization energy λ_p can be rewritten as

$$\lambda_p=\lambda^L+\lambda^T-\lambda^{\mathrm{corr}}, \tag{83}$$

where

$$\lambda^{L,T}=\frac{3y_p}{8\pi}|\Delta\tilde{E}_0^{L,T}|^2*S^{L,T}. \tag{84}$$

The correction term λ^{corr} accounts for the modification of the polarization response by the presence of the solute. It can be written in the form avoiding the convolution in the inverted space as follows:

$$\lambda^{\mathrm{corr}}=\frac{3y_p}{8\pi}\int_{\Omega_0}\Delta\mathbf{E}_0'(\mathbf{r})\cdot\Delta\mathbf{E}_0''(\mathbf{r})d\mathbf{r}, \tag{85}$$

where the new effective fields $\Delta\mathbf{E}_0'$ and $\Delta\mathbf{E}_0''$ are the inverse Fourier transforms of the expressions

$$\Delta\tilde{\mathbf{E}}_0'(\mathbf{k})=\hat{\mathbf{k}}\Delta\tilde{E}_0^L(\mathbf{k})(S^L(k)-S^T(k))+\Delta\tilde{\mathbf{E}}_0(\mathbf{k})S^T(k) \tag{86}$$

and

$$\begin{aligned}\Delta\tilde{\mathbf{E}}_0''(\mathbf{k})=&\hat{\mathbf{k}}\Delta\tilde{E}_0^L(\mathbf{k})[(\chi'')^L(k)-(\chi'')^T(k)]\\&+\Delta\tilde{\mathbf{E}}_0(\mathbf{k})(\chi'')^T(k).\end{aligned} \tag{87}$$

The main challenge in practical applications of the present formalism is the calculation of the function $\boldsymbol{\chi}'$. We provide here an approximate derivation applicable to solutes which are large compared to the solvent molecules. The integration over $\mathbf{k}$ in Eq. (78) yields

$$\boldsymbol{\chi}'(\mathbf{k})=\int_{\Omega'}d\mathbf{r}\,e^{i\mathbf{k}\cdot\mathbf{r}}\left[\left(\delta(\mathbf{r})+\frac{\rho}{3}h^{110}(r)\right)\mathbf{1}+\frac{\rho}{3}h^{112}(r)\mathbf{D}_\mathbf{r}\right], \tag{88}$$

with $\mathbf{D}_\mathbf{r}=3\hat{\mathbf{r}}\hat{\mathbf{r}}-\mathbf{1}$. In the above integral, only the long-range 112 component survives for large solutes. The asymptotic form of $h^{112}(r)$ can be found from Eq. (32) as

$$\rho h^{112}(r)\simeq\frac{c_0^2\epsilon_s}{4\pi y_p}\frac{1}{r^3}. \tag{89}$$

When Eq. (89) is used in Eq. (88), one obtains

$$\boldsymbol{\chi}'(\mathbf{k})=\frac{c_0^2\epsilon_s}{12\pi y_p}\int_{\Omega'}\frac{\mathbf{D}_\mathbf{r}}{r^3}e^{i\mathbf{k}\cdot\mathbf{r}}d\mathbf{r}. \tag{90}$$

This expression represents the Fourier transform of the rank-2 tensor corresponding to a point dipole placed at the center of the cavity formed by the region Ω_0'. When the solute is a spherical cavity of the radius R_1 the solution is

$$\boldsymbol{\chi}'(\mathbf{k})=-2A(k)\mathbf{J}^L+A(k)\mathbf{J}^T, \tag{91}$$

with

$$A(k)=\frac{c_0^2\epsilon_s}{3y_p}\frac{j_1(2kR_1)}{2kR_1}. \tag{92}$$

From Eq. (91) the function $\boldsymbol{\chi}''$ in Eq. (82) becomes

$$\boldsymbol{\chi}''=\mathbf{J}^L\frac{S^L}{S^L+2A}+\mathbf{J}^T\frac{S^T}{S^T-A}. \tag{93}$$

At $k=0$, $S^L(0)+2A(0)=S^T(0)-A(0)=g_K$ [Eq. (33)] and $\boldsymbol{\chi}''$ turns into $g_K^{-1}\boldsymbol{\chi}_s$ in the continuum limit. The function $\boldsymbol{\chi}''$ from Eq. (93) can be used in Eq. (87) to obtain the correction of solvent's polarization response by solute's repulsive core. Before turning to a general solution, we first consider a simpler case of a dipolar spherical solute for which an exact analytical solution is possible.[116]

A. Dipolar solute

An exact solution for λ_p can be obtained for a point dipole approximation for the field of ET dipole. When, in addition, the solute is represented by a sphere of an effective radius R_0, $\Delta\tilde{\mathbf{E}}_0$ is given by the relation

$$\Delta\tilde{\mathbf{E}}_0(\mathbf{k})=-4\pi\mathbf{m}_0\cdot\mathbf{D}_\mathbf{k}\frac{j_1(kR_1)}{kR_1}, \tag{94}$$

where $\mathbf{D}_\mathbf{k}=3\hat{\mathbf{k}}\hat{\mathbf{k}}-\mathbf{1}$ and $\mathbf{m}_0$ is the ET dipole moment. From Eqs. (87) and (93) the field $\Delta\mathbf{E}_0''$ is the inverse Fourier transform given as

$$\Delta\mathbf{E}_0''(\mathbf{r})=\int\frac{d\mathbf{k}}{(2\pi)^3}[S_1\hat{\mathbf{k}}\Delta\tilde{E}_0^L+S_2\Delta\tilde{\mathbf{E}}_0]e^{-i\mathbf{k}\cdot\mathbf{r}}, \tag{95}$$

where

$$S_1=\frac{S^L}{S^L+2A}-\frac{S^T}{S^T-A}, \tag{96}$$

$$S_2=\frac{S^T}{S^T-A}.$$

Since the space integral in $\lambda^{\rm corr}$ [Eq. (85)] is taken over the solute volume, one needs to calculate the above integral for $r\leqslant R_1$ only. The integral is calculated by complex k-plane integration. The functions $S^L/(S^L+2A)$ and $S^T/(S^T-A)$ do not have singularities in the complex k plane since existing singularities of $S^{L,T}$ cancel out in the nominator and denominator.[117] Therefore, only the $k=0$ pole of $\Delta\tilde{E}_0$ contributes to the integral. The result of integration within the solute sphere, $r<R_1$ is then a constant field:[116]

$$\Delta\mathbf{E}_0''=\frac{2\mathbf{m}_0}{3g_K R_1^3}[S^T(0)-S^L(0)]. \tag{97}$$

This result greatly simplifies the solution for $\lambda^{\rm corr}$, which becomes

$$\lambda^{\rm corr}=\frac{S^T(0)-S^L(0)}{3g_K}[2\lambda^T-\lambda^L]. \tag{98}$$

From Eqs. (83) and (98), the reorganization energy λ_p is

$$\lambda_p=g_K^{-1}S^T(0)\lambda^L+g_K^{-1}S^L(0)\lambda^T. \tag{99}$$

When λ^L and λ^T [Eq. (84)] are calculated in the continuum limit by assuming $S^{L,T}(k)=S^{L,T}(0)$ one arrives at the solution

$$\lambda_p=\frac{m_0^2}{R_1^3}\frac{\epsilon_s-\epsilon_\infty}{\epsilon_\infty^2(2\epsilon_s+\epsilon_\infty)}. \tag{100}$$

Equation (100) transforms into the Onsager form in Eq. (39) when $\epsilon_\infty=1$.

Equation (99) presents an exact solution for λ_p of ET in an arbitrary dielectric material characterized by longitudinal and transverse structure factors when $\Delta\mathbf{E}_0$ is approximated by the point dipole field. The convergence of Eq. (99) into the Onsager continuum limit indicates that the NRFT does resolve the problem of a ''transverse catastrophe'' posed by direct perturbation expansions.[116] The continuum limit of the NRFT [Eq. (100)] yields a significantly stronger dependence of λ_p on ϵ_∞ than the one suggested by the Lippert–Mataga (superscript ''LM'') equation.[100] The latter predicts that λ_p is proportional to the polarity parameter

$$f_p^{\rm LM}=\frac{\epsilon_s-1}{2\epsilon_s+1}-\frac{\epsilon_\infty-1}{2\epsilon_\infty+1}. \tag{101}$$

Equation (101) is based on the assumption that electronic and nuclear solvations additively contribute to the total solvation free energy. The numerical accuracy of this assumption is supported by MC simulations of dipolar solvation in polarizable solvents.[65] However, compared to both liquid-state theories and simulations, the Lippert–Mataga equation greatly overestimates the falloff of λ_p with increasing ϵ_∞ (Ref. 65).

The continuum limit of the NRFT allows us to draw two conclusions. First, the additive approximation is not exact. Second, the continuum λ_p in Eq. (100) depends more strongly on ϵ_∞ than the Lippert–Mataga equation suggests.

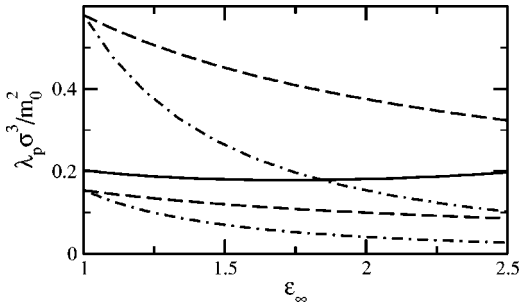

FIG. 12. λ_p vs ϵ_∞ calculated in the NRFT [Eq. (99), solid line], in its continuum limit [Eq. (100), dash-dotted lines], and from the Lippert–Mataga equation [Eq. (101), dashed lines]. For the dashed-dotted and dashed lines, the upper curves refer to the vdW radius R_0 and the lower curves refer to the SA radius R_1. For a given ϵ_∞, the solvent polarizability is calculated from the Clausius–Mossotti equation, the effective dipolar density is obtained from the Wertheim 1-RPT theory, and the static dielectric constant is obtained from y_e+y_p according to Eq. (102); $R_0/\sigma=0.9$ and $\rho=0.8$.

For instance, increasing ϵ_∞ from 1 to 2 at $\epsilon_s\gg 1$ leads to a decrease in λ_p by a factor of 1.7 according to Eq. (101) and by a factor of 4.0 according to Eq. (100) (cf. dashed and dash-dotted lines in Fig. 12). On the other hand, when ϵ_∞ is varied between 1 and 2 in the microscopic formulation, the reorganization energy λ_p essentially does not change (solid line in Fig. 12). In the calculation presented in Fig. 12, the solvent permanent dipole is held constant while ϵ_∞ is varied. The change in ϵ_∞ is microscopically caused by a change in the solvent polarizability α connected to ϵ_∞ by the Clausius–Mossotti equation. The increase in the polarizability leads to an increase in the solvent dielectric constant due to two effects: a higher condensed-phase dipole moment (main contribution) and a higher density of induced dipoles $y_e=(4\pi/3)\rho\alpha$. The dielectric constant is then calculated by using the equation based on the perturbation expansion for the Kirkwood factor:[47]

$$\epsilon_s(y_{\rm eff})=1+3y_{\rm eff}+3y_{\rm eff}^2+\frac{2}{p^2}[\exp(3p^3y_{\rm eff}^3/2)-1], \tag{102}$$

where

$$y_{\rm eff}=y_p+y_e \tag{103}$$

is the effective, mean-field density of dipoles in a polar-polarizable solvent[45] and $p=9I_{dd\Delta}(\rho^*)/16\pi^2-1$; $I_{dd\Delta}(\rho^*)$ is the perturbation integral[118] depending on the reduced solvent density $\rho^*=\rho\sigma^3$. The calculations in Fig. 12 are carried out for a relatively weakly polar solvent with $m^*=1$ for which Eq. (102) compares well to MC simulations.[47] The main result of the calculations presented in Fig. 12 can be summarized as follows. The microscopic formulation predicts λ_p almost independent of ϵ_∞, in qualitative agreement with MC simulations of solvation in dipolar-polarizable fluids[65] and earlier force-field simulations.[119] A direct transition from the microscopic formulations to the continuum limit leads to Eq. (100) in which the additive approximation of the Lippert–Mataga equation is not present. However, this transition results in an inadequate dependence of λ_p on ϵ_∞.

B. Solute of arbitrary shape

Equations (83)–(87) formally solve the problem of reorganization energy calculations for solutes of arbitrary shape. The procedure is, however, unstable numerically since λ^T and λ^{corr} are two large numbers canceling each other almost identically in Eq. (83). Errors in calculating each of them do not cancel out, making the calculations impractical for $y \geqslant 1.5$. The problem is well illustrated by the exact solution for dipolar solutes. The component λ^T in Eq. (83) and the transverse component in λ^{corr} together result in $g_K^{-1}S^L(0)\lambda^T$ [Eq. (99)]. The latter becomes negligible in highly polar solvents. The first summand in Eq. (99) then leads to the approximate relation

$$\lambda_p \simeq \frac{3}{2}\lambda^L. \tag{104}$$

We will use the solution for a dipolar solute to formulate a consistent, numerically stable calculation scheme for a solute of arbitrary shape.

The field $\Delta\mathbf{E}_0''(\mathbf{r})$ which enters λ^{corr} [Eq. (85)] can be expanded in spherical harmonics $Y_{nm}(\hat{\mathbf{r}})$ by using the Rayleigh expansion for the plane wave $\exp(-i\mathbf{k}\cdot\mathbf{r})$ (Ref. 57) in Eq. (95). This yields

$$\Delta\mathbf{E}_0''(\mathbf{r}) = \sum_{n,m} \mathbf{F}_{nm}(r) Y_{nm}^*(\hat{\mathbf{r}}), \tag{105}$$

where

$$\mathbf{F}_{nm}(r) = \frac{(-i)^n}{\pi}\int_{-\infty}^{\infty} dk\, k^2 j_n(kr)[S_1\langle \Delta\tilde{E}_0^L \hat{\mathbf{k}} Y_{nm}(\hat{\mathbf{k}})\rangle_{\omega_k} + S_2\langle \Delta\tilde{\mathbf{E}}_0 Y_{nm}(\hat{\mathbf{k}})\rangle_{\omega_k}]. \tag{106}$$

In Eq. (106), $\langle\cdots\rangle_{\omega_k}$ stands for the angular average over the orientations of $\hat{\mathbf{k}}$. Since $S_2(k)$ in Eq. (96) does not have poles in the complex k plane, it is easy to show that the integral of the second summand in the brackets in Eq. (106) is identically zero. This is not the case for the first summand including the longitudinal component of $\Delta\tilde{\mathbf{E}}_0$.

The $n=0$ component of the sum over n in Eq. (106) can be used to formulate a computationally efficient mean-field solution avoiding the problem of mutual cancellation of large transverse components in λ^T and λ^{corr}. Similarly to the case of a dipolar solute [Eq. (97)], the $n=0$, $m=0$ projection $\mathbf{F}_{00}(r)=\mathbf{F}_0$ is independent of r within the solute:

$$\mathbf{F}_0 = \frac{S^T(0)-S^L(0)}{4\pi g_K}\int_\Omega \Delta\mathbf{E}_0\cdot\mathbf{D}_{\mathbf{r}}\frac{d\mathbf{r}}{r^3}. \tag{107}$$

Equation (107) bears a very clear physical meaning. Placing a charge within a spherical dielectric cavity creates a constant cavity potential, but zero cavity field. The dipole at the center of a spherical cavity induces a solvent polarization, which creates a constant reaction field within the cavity. The dipolar projection of an arbitrary solute field in Eq. (107) clearly creates a constant reaction field $\mathbf{F}_0$. Higher-order terms with $n, m>0$ are responsible for nonzero gradients of the reaction field.

It may be reasonable to assume that gradients of the reaction field are less important in the solvation free energy than the average reaction field within the cavity. One can build a mean-field solution based on this assumption. In fact, numerical calculations of the field $\Delta\mathbf{E}_0''$ show that it is independent of $\mathbf{r}$ within the solute, but its magnitude is somewhat shifted from the result of Eq. (107). In order to accommodate for this fact, we replace $\Delta\mathbf{E}_0''$ with $a^{\mathrm{MF}}\mathbf{F}_0$, where the mean-field coefficient a^{MF} is chosen from the requirement that λ^{corr} renormalizes λ^T to $[S^L(0)/g_K]\lambda^T$ in Eq. (83). This yields

$$a^{\mathrm{MF}}\frac{3y_p}{8\pi}\mathbf{F}_0\cdot\int\frac{d\mathbf{k}}{(2\pi)^3}\theta^*(\mathbf{k})\Delta\tilde{\mathbf{E}}_0^T(\mathbf{k}) = f_p\lambda^T, \tag{108}$$

where $\Delta\tilde{\mathbf{E}}_0^T = \Delta\tilde{\mathbf{E}}_0 - \hat{\mathbf{k}}\Delta\tilde{E}_0^L$ and

$$f_p = \frac{2(S^T(0)-S^L(0))}{3g_K} = \frac{2(\epsilon_s-\epsilon_\infty)}{2\epsilon_s+\epsilon_\infty} \tag{109}$$

is the reaction-field factor for continuum nuclear solvation of a dipole in a spherical cavity.

The mean-field (superscript "MF") solution for the orientational reorganization energy then becomes

$$\lambda_p^{\mathrm{MF}} = g_K^{-1}S^L(0)\lambda^T + \frac{3y_p}{8\pi}\int\frac{d\mathbf{k}}{(2\pi)^3}S^L(k) \times\left[|\Delta\tilde{E}_0^L|^2 - f_p|\Delta\tilde{E}_0^T|^2\frac{\mathbf{F}_0\cdot\hat{\mathbf{k}}\Delta\tilde{E}_0^L}{\mathbf{F}_0\cdot\Delta\tilde{\mathbf{E}}_0^T}\right]. \tag{110}$$

There are several advantages to this equation: First, it reduces the calculation of λ_p to a three-dimensional (3D) integral in the inverted space. Second, the errors of approximate calculations are not amplified in the transverse reorganization component which becomes insignificant in highly polar solvents [first summand in Eq. (110)]. Third, Eq. (110) transforms into the exact solution of Eq. (99) for the dipolar solute and gives $\lambda_p=\lambda^L$ for solutes with purely longitudinal fields (e.g., spherical ions). Therefore, Eq. (110) correctly reproduces the two limiting cases of longitudinal and dipolar solute fields and provides a mean-field solution between them. It also splits λ_p into its longitudinal and transverse components, which allows us to draw qualitative conclusions about the relative importance of these two collective modes in activating ET.

With the account for the mean-field result, the exact solution for λ_p is given by the relation

$$\lambda_p = \lambda_p^{\mathrm{MF}} - \delta\lambda^{\mathrm{corr}}, \tag{111}$$

where the correction term accounts for of the deviation of the total field $\Delta\mathbf{E}_0''$ from the mean-field result $a^{\mathrm{MF}}\mathbf{F}_0$ [cf. to Eq. (85)]:

$$\delta\lambda^{\mathrm{corr}} = \frac{3y_p}{8\pi}\int_{\Omega_0}\Delta\mathbf{E}_0'\cdot(\Delta\mathbf{E}_0''-a^{\mathrm{MF}}\mathbf{F}_0)d\mathbf{r}. \tag{112}$$

Calculations according to Eqs. (110)–(112) for ET reorganization in model donor–acceptor diatomics, as well as the comparison to computer simulations, are given in Sec. VI below following analytical formulation of the solvent structure factors necessary for the inverted-space integration.

V. STRUCTURE FACTORS

The use of the charge–dipole approximation for the solute–solvent interaction potential [condition (48)] yields the solvation thermodynamics in terms of the longitudinal and transverse polarization structure factors defined by Eqs. (24) and (25). They can be expanded in rotationally invariant projections of the solvent–solvent pair correlation function $h_{ss}(12)$. Using the Rayleigh expansion[57] in Eq. (24), one gets for $S^L(k)$

$$S^L(k)=1+12\pi\rho\sum_{n,m} i^n Y^*_{nm}(\hat{\mathbf{k}})\int (\hat{\mathbf{e}}_1\cdot\hat{\mathbf{k}}) \times(\hat{\mathbf{k}}\cdot\hat{\mathbf{e}}_2) j_n(kr_{12}) Y_{nm}(\hat{\mathbf{r}}_{12}) h_{ss}(r_{12},\omega_1,\omega_2) d\mathbf{r}_{12} \times\frac{d\omega_1 d\omega_2}{(4\pi)^2}, \tag{113}$$

where ω_1 and ω_2 refer to orientations of dipoles 1 and 2, respectively. For solvent molecules with axial symmetry one can expand $h_{ss}(12)$ in spherical harmonics:

$$h_{ss}(12)=\sum_{l_1 l_2 l} h_{ss}(l_1 l_2 l;r_{12}) \sum_{m_1 m_2 m} C(l_1 l_2 l;m_1 m_2 m) \times Y_{l_1 m_1}(\hat{\mathbf{e}}_1) Y_{l_2 m_2}(\hat{\mathbf{e}}_2) Y^*_{lm}(\hat{\mathbf{r}}_{12}), \tag{114}$$

where $C(l_1 l_2 l;m_1 m_2 m)$ are Clebsh–Gordon coefficients generating a rotationally invariant linear combination of the products of three Y_{lm}'s. The integration in Eq. (113) then leads to the expansion

$$S^L(k)=1+\frac{\rho}{(4\pi)^{3/2}} \times\sum_{m=0}^{\infty}\sqrt{4m+1}\,C(11(2m);000)\hat{h}^{11(2m)}_{ss}(k), \tag{115}$$

where $\hat{h}^{11(2m)}_{ss}(k)$ is the Hankel transform:

$$\hat{h}^{11(2m)}_{ss}(k)=4\pi(-1)^m\int_0^\infty h_{ss}(l_1 l_2(2m);r) j_{2m}(kr) r^2 dr. \tag{116}$$

The transverse structure factor is obtained from Eqs. (115) and (117):

$$\frac{1}{3}S^L(k)+\frac{2}{3}S^T(k)=1-\frac{\rho}{\sqrt{3}(4\pi)^{3/2}}\hat{h}^{110}_{ss}(k). \tag{117}$$

The Clebsh–Gordon coefficient $C(11(2m),000)$ is nonzero only for $m=0$ and $m=1$, leading to the structure factors in terms of projection of $h_{ss}(12)$ on rotational invariants:

$$S^L(k)=1+(\rho/3)[\tilde{h}^{110}_{ss}(k)+2\tilde{h}^{112}_{ss}(k)] \tag{118}$$

and

$$S^T(k)=1+(\rho/3)[\tilde{h}^{110}_{ss}(k)-\tilde{h}^{112}_{ss}(k)]. \tag{119}$$

Here $\tilde{h}^{110}_{ss}$ and $\tilde{h}^{112}_{ss}$ are the projections on rotational invariants $\Delta(12)=(\hat{\mathbf{e}}_1\cdot\hat{\mathbf{e}}_2)$, projection (110), and $D_k(12)=3(\hat{\mathbf{e}}_1\cdot\hat{\mathbf{k}}) \times(\hat{\mathbf{k}}\cdot\hat{\mathbf{e}}_2)-(\hat{\mathbf{e}}_1\cdot\hat{\mathbf{e}}_2)$, projection (112), respectively. They are related to $\hat{h}^{11n}_{ss}(k)$ by numerical coefficients: $\tilde{h}^{110}_{ss}=-\sqrt{3}(4\pi)^{-3/2}\hat{h}^{110}_{ss}$ and $\tilde{h}^{112}_{ss}=\sqrt{15/2}(4\pi)^{-3/2}\hat{h}^{112}_{ss}$.

Equations (118) and (119) are used in the literature[59] to produce dipolar structure factors from the corresponding radial distribution functions obtained from computer simulations for molecular fluids with site–site interaction potentials. This approach incorporates a realistic charge distribution within solvent molecular cores instead of relying on the point–dipole (PD) approximation. The PD approximation is based on the assumption of smallness of the parameter

$$\zeta_2=l_{ss}/\sigma\ll 1. \tag{120}$$

This condition is usually much less accurate than the condition for application of the charge–dipole approximation to the solute–solvent potential [Eq. (48)]. In fact, molecular quadrupoles are very effective in breaking the dipole–dipole correlations in polar liquids,[45,46] resulting in dielectric constants much smaller (lower Kirkwood factor g_K) than for purely dipolar solvents (Table I). This feature is by far more important for the calculation of λ_p than the breakdown of the point–multipole model at large values of $k\geqslant 2\pi/l_{ss}$ (Ref. 22).

Table I presents the results of MC simulations of pure dipolar liquids of increasing polarity (m^*) and the same set of data for fluids with a constant axial quadrupole moment Q characterized by the reduced value $(Q^*)^2=\beta Q^2/\sigma^5=0.5$ [$(Q^*)^2=0.2$, 0.7, and 0.2 for acetone, dimethylsulfoxide, and tetrahydrofurane, respectively]. The simulations were carried out as explained in Refs. 36 and 47 and in Appendix A. Figures 7 and 13 present the polarization longitudinal and density structure factors calculated from simulations for dipolar liquids. Figure 14 shows the transverse structure factors calculated for purely dipolar liquids (upper panel) and for dipolar–quadrupolar liquids (lower panel).

For both dipolar and dipolar–quadrupolar fluids, the transverse structure factor at $k=0$ increases with increasing solvent dipole m. The inclusion of the quadrupole moment does not change this picture, but slows down the growth of $S^T(0)$ (Table I and Fig. 14). The function $S^T(k)$ becomes thus increasingly narrow with increasing solvent polarity approaching the ferroelectric singularity $S^T(0)\to\infty$ at $y\to\infty$ predicted by the MSA and mean-field theories.[110] This property of the transverse structure factor turns out to be important for the disappearance of the microscopic transverse response from the solvent reorganization energy (see below).

In view of the substantial effect of higher molecular multipoles on the behavior of $S^{L,T}(k)$ at $k\to 0$, the PD approximation is not applicable to the calculation of polarization structure factors of molecular liquids. These functions are not accessible experimentally, and computer simulations and/or liquid-state theories should be used on multipolar or interaction-site model potentials. Simulations of structure factors are time consuming due to the long-range character of polarization fluctuations and only a few systems have been studied so far.[58,59,101–104] It seems, however, true that, in the range of k vectors affecting the value of λ_p, the behavior

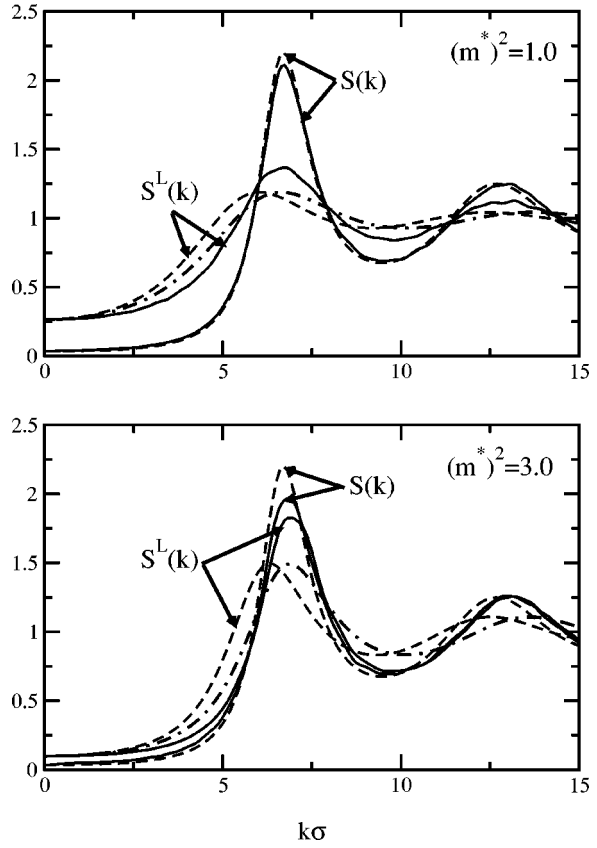

FIG. 13. Density structure factor $[S(k)]$ and the longitudinal polarization structure factor $[S^L(k)]$ calculated from MC simulations at $(m^*)^2=1.0$ and 3.0 (solid lines). The dashed lines indicate the PY (density) and PPSF (polarization) calculations. The dashed lines refer to the PPSF $S^L(k)$ from Eq. (126) with $\kappa=1.0$ and the dot-dashed lines refer to $\kappa=0.95$.

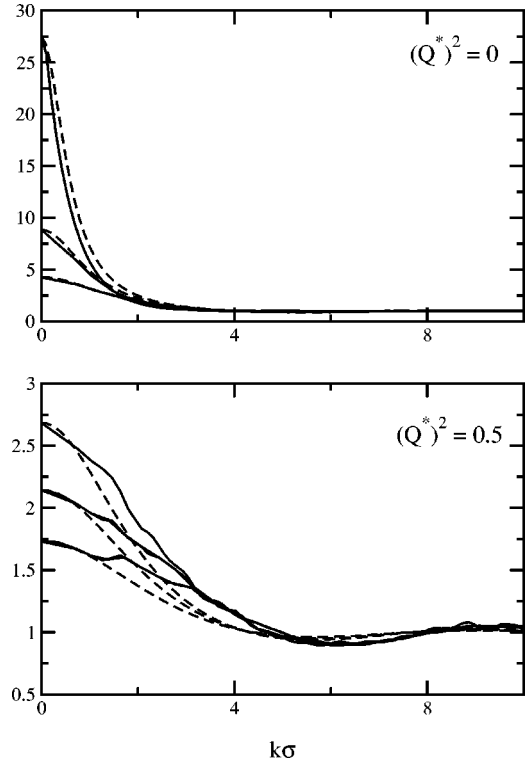

FIG. 14. $S^T(k)$ from MC simulations (solid lines) at $(m^*)^2=2.0$, 3.0, and 4.0 (from the lower to the upper curve) for dipolar liquids (upper panel) and dipolar–quadrupolar liquids with $(Q^*)^2=0.5$ (lower panel). The dashed lines indicate calculations with the PPSF; $\rho^*=0.8$.

of the polarization structure factors is not greatly sensitive to the details of the solvent molecular structure, showing a generic pattern characteristic of many molecular liquids. It would therefore be desirable to parametrize an existing analytical solution for structure factors to a simple route consistent with computer simulations and reproducing the long-wavelength polarization response of real solvents significant for reorganization energy calculations in terms of experimental input parameters.

A very attractive approach to the calculation of $S^{L,T}(k)$ is to apply the analytical MSA solution. The Wertheim's MSA result for the solvent of dipolar HS molecules[83] sets up $S^{L,T}(k)$ in terms of the Baxter factorization function $Q(k\sigma)$ (Ref. 57) as

$$S^{L,T}(k)=|Q^{L,T}(k\sigma)|^{-2}. \tag{121}$$

The function

$$Q^{L,T}(k\sigma)=1-A^{L,T}\int_0^1 e^{ik\sigma t}[(t^2-1)/2-\Lambda^{L,T}(t-1)]dt \tag{122}$$

is given in terms of $S^{L,T}(0)$ and the correlation length $\Lambda^{L,T}$, where

$$A^{L,T}=6\,\frac{1/\sqrt{S^{L,T}(0)}-1}{2-3\Lambda^{L,T}}. \tag{123}$$

The MSA defines $S^{L,T}(k)$ through a single polarity parameter ξ that can be connected either to the dipolar density y_p and ϵ_∞ or to two dielectric constants ϵ_s and ϵ_∞ by applying the MSA solution for the Kirkwood factor $g_K(y_p)$. The MSA result for $g_K(y_p)$ is, however, unrealistic for molecular liquids.[47] A way around this complication is to consider y_p and two dielectric constants as independent input parameters. This route sets up a three-parameter definition of the nuclear polarization structure factors. Since the dipolar correlation lengths are not available from experiment and are also very hard to obtain from computer simulations,[105] we will use the MSA prescription to calculate $\Lambda^{L,T}$. This approach is most easily formulated by introducing two polarity parameters ξ^L and ξ^T for $S^L(k)$ and $S^T(k)$ separately. Each parameter is defined by the condition that $|Q^{L,T}(0)|^{-2}$ generate $S^{L,T}(0)$ given by the MSA solution[83]

$$\frac{(1-2\xi^L)^4}{(1+4\xi^L)^2}=S^L(0),$$
$$\frac{(1+\xi^T)^4}{(1-2\xi^T)^2}=S^T(0). \tag{124}$$

Dielectric constants from experiment or simulations can be used in Eqs. (32) and (124) to calculate $S^{L,T}(0)$ and $\xi^{L,T}$. For the parameter y_p, Wertheim's 1-RPT self-consistent scheme[66] allows one to calculate solution dipole moments in a broad range of solvent polarities.[65] The parameters ξ^L and ξ^T obtained from Eq. (124) are then used in Eqs. (21) and (22), respectively, to define the correlation lengths for longi-

tudinal and transverse fluctuations. We will refer to $S^{L,T}(k)$ obtained from the MSA solution with a separate definition of the polarity parameters for longitudinal and transverse structure factors through y_p, ϵ_∞, and ϵ_s as the parametrized polarization structure factors (PPSFs). This approach is qualitatively analogous to the parametrization of the RISM closure relations in terms of ϵ_s and y (Ref. 120) by the requirement of reproducing the $k=0$ limit for the polarization structure factors.[29]

An alternative approach to parametrize the polarization structure factors is to apply the exact relations connecting $S^{L,T}(k)$ to the average energy u_{ss} of dipole–dipole interactions in dipolar solvents:

$$\int (S^L(k)-1)\frac{d\mathbf{k}}{(2\pi)^3}=\frac{\beta u_{ss}}{3y_p}\rho,$$
$$\int (S^T(k)-1)\frac{d\mathbf{k}}{(2\pi)^3}=-\frac{\beta u_{ss}}{6y_p}\rho. \tag{125}$$

These equations can be used to define the correlation length in Eqs. (121) and (122) provided the interaction energy u_{ss} is known from simulations or analytical models. We found, however, that this route does not offer any significant advantages compared to the PPSFs. Equation (125) may, however, be used as a consistency test for structure factors generated from computer simulations.

As is seen in Fig. 13, the MSA solution gives the first maximum of $S^L(k)$ shifted to lower values of k compared to the simulation results. The position of the first maximum of $S^L(k)$ from simulations is practically independent of y shifting only slightly to higher k with increasing y. The maxima of the density and longitudinal polarization structure factors essentially coincide in a broad range of solvent polarities. Evidently, this has to be related to the fact that the centers of charge and mass coincide for multipolar HS molecules. The distribution of mass and charge may not coincide for asymmetric solvent molecules, resulting in a shift between first maxima of $S^L(k)$ and $S(k)$. A better agreement between the PPSFs and simulations can be achieved by a downward rescaling of σ in the Baxter function in Eq. (122) used for $S^L(k)$. Specifically, the use of

$$S^L(k)=|Q^L(\kappa k\sigma)|^{-2}, \tag{126}$$

with $\kappa=0.95$, shifts the first maximum of $S^L(k)$ to the right position. Still existing discrepancies between $S^L(k)$ from simulations and PPSFs do not affect the value of λ_p (see below). It also turns out that Eq. (121) for $S^T(k)$ and Eq. (126) for $S^L(k)$ work well for dipolar–quadrupolar solvents (Figs. 7 and 14). Figure 13 shows that Baxter's solution of the PY equation for HS liquids[57,121] gives $S(k)$ in good agreement with MC simulations of polar solvents. This form of $S(k)$ is used for the calculation of the density reorganization energy below.

The PPSF may appear to be a reasonable approximation for the dipolar-symmetry structure factors of real molecular liquids. Figure 15 compares the longitudinal (L) and transverse (T) structure factors from the PPSF and from simulations of the model DMSO with an interaction-site potential

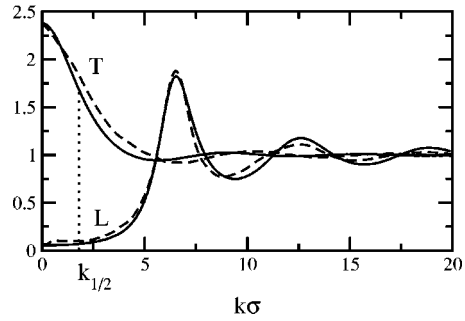

FIG. 15. Comparison between the longitudinal (L) and transverse (T) structure factors calculated by the PPSF (solid lines) and obtained from MD simulations of DMSO with an interaction-site potential (Ref. 59) (dashed lines). The MD structure factors as functions of k are scaled with $\sigma=4.73$ Å for comparison with the PPSF results given in the $k\sigma$ scale. The dotted line labeled $k_{1/2}$ defines the characteristic decay length of $S^T(k)$ used to derive the criterion of applicability of continuum models in Eq. (130).

($y=6.08$, $\epsilon_\infty=1.0$, $\epsilon_s=44.4$).[59] Since the HS diameter is not defined in the interaction-site model, the simulated k vectors were multiplied by $\sigma=4.73$ Å to obtain the $k\sigma$ scale of the PPSF model.[122] The scaling was chosen to make the positions of the first maxima of $S^L(k)$ in two calculations coincide.

VI. RESULTS AND DISCUSSION

The formalism developed in Secs. IV and V is compared here to MC simulations described in Sec. II and Appendix A. We begin with the description of the numerical algorithm.

A. Calculation procedure

Numerical implementation of the analytical formalism includes two components: (i) the calculation of the Fourier transform of the electric field of the ET dipole (Fig. 1) and (ii) the calculation of the response function and 3D integration in the inverted space [Eqs. (99) and (110)]. The Fourier transform of the electric field created by the ET dipole is taken over the solvent-accessible volume [Eq. (3)]. It can be calculated for an arbitrary solute shape by employing fast Fourier transform (FFT) techniques[123] on a grid of direct-space points. A direct numerical calculation is, however, not possible because of the conditional convergence of the Fourier integral of the Coulomb field. The problem is overcome by splitting the solvent volume into two regions: the region between the DAC and a sphere enclosing it and a region outside the sphere. The Fourier integral inside the sphere is taken numerically by the FFT and the Fourier integral outside the sphere is calculated analytically (Appendix C).

The polarization structure factors directly from MC simulations and the PPSF were used in Eqs. (99) and (110) to calculate λ_p. The two sets of calculations give essentially indistinguishable results, and all the calculations are carried out with the use of the PPSF. The density reorganization energy was calculated from Eq. (67) with the density structure factor from the PY solution for the HS fluid.[121] Specifically, the convolution integral in the inverted space in Eq. (67) has been avoided by calculating $\theta_0(\mathbf{k})$, taking the inverse Fourier transform (F^{-1}) of $[S(k)-1]\theta_0(\mathbf{k})$,

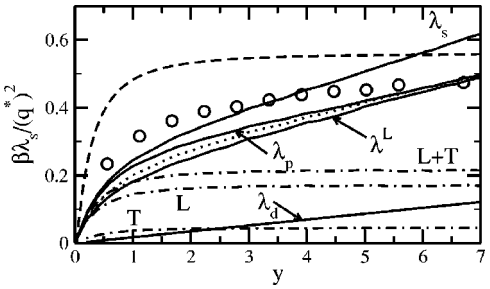

FIG. 16. λ_s for a charged diatomic from the Marcus equation [Eq. (38), dashed line], MC simulations (circles), and the NRFT (solid lines). The dotted line shows the longitudinal component of λ_p obtained by 3D integration with the longitudinal structure factor [second summand in Eq. (110)]. λ^L refers to the longitudinal reorganization energy in Eq. (84). The dot-dashed lines refer to the continuum limits for of the longitudinal ("L") and transverse ("T") components of λ_s^{MF} obtained by setting the polarization structure factors to their $k=0$ values. "L+T" refers to the continuum λ_s^{MF}. The dashed line is the Marcus formula for a DAC diatomic [Eq. (38)]; $R_A=R_D=0.9\sigma$, $R=1.8\sigma$, $\rho^*=0.8$, and $Q^*=0.0$.

$$\mathcal{F}(\mathbf{r})=F^{-1}[(S(k)-1)\theta_0(\mathbf{k})], \tag{127}$$

and calculating the direct-space integral

$$\lambda_d=-\frac{3y_p}{8\pi}\mathcal{F}*\Delta\mathbf{E}_0^2. \tag{128}$$

The calculations of λ_p and λ_s were carried out at varying y [Eq. (15), nonpolarizable solvent] for two solute geometries for which MC simulation data are available: point dipole and diatomic.

B. Comparison of the analytical model to MC simulations

Figure 10 compares the result of MC simulation for the LRA λ_s with the results of calculation for a dipolar solute [Eqs. (99) and (128)]. The solid points and solid lines refer to the results of calculations using structure factors from MC simulations and the PPSF/PY, respectively. As is seen, the PPSF solution for the polarization structure factors and the PY HS solution for the density structure factor provide sufficient accuracy for the purpose of reorganization energy calculations. At low polarities, the simulated λ_s (open points) deviates somewhat upward from analytical calculations and the analytical results tend to be higher at large polarities. The same qualitative picture is observed for the comparison between simulations and calculations performed for the diatomic DAC in the contact configuration as shown in Fig. 16. The calculation of the full λ_p [Eq. (111)] turns out to fall within 1% of the mean-field solution. For all practical purposes, the mean-field result provides sufficient accuracy for the calculations of λ_p. One possible reason for the observed deviation between the analytical calculations and MC simulations is that the density reorganization energy has been calculated here from a perturbative solution[20] without attempting to perform a complete renormalization similar to that achieved for the orientational component. Further theory development in this direction is necessary.

The Marcus equation for ET diatomic [Eq. (38), dashed line in Fig. 16] is in a reasonable agreement with simulation results at high solvent polarities, $y>6$. The dependence on solvent polarity is obviously not reproduced by the Marcus equation, and one should avoid applying it for analyzing solvent polarity effects on λ_s. In addition, Eq. (38) does not correctly reproduce the dependence of λ_s on ϵ_∞ (Ref. 65) (see below).

C. Qualitative results

On the qualitative level, a significant finding of this study is the understanding of the role of transverse and longitudinal polarization fluctuations as collective solvent modes driving ET. We have shown that longitudinal solvent polarization dominates the microscopic solvent response. The transverse response essentially disappears from solvation energetics at high solvent polarities (cf. dotted and solid lines in Fig. 16). It is important to realize that the disappearance of the transverse response is purely a microscopic effect not present in continuum formulations of the theory. Indeed, when the continuum approximation $S^T(k)\simeq S^T(0)$ is made in the calculation of λ^T in Eqs. (99) and (110), the transverse contribution to the reorganization energy is quite substantial, $c_0\mathcal{E}_0^T/2$ at large y (cf. continuum longitudinal, "L," and transverse, "T," reorganization energies shown by dash-dotted lines in Fig. 16). The transverse component disappears in the microscopic calculations because of the strong decay of the transverse structure factor at $k\sigma<\pi$ in highly polar solvents (Fig. 14). This result resolves the puzzling contradiction between electrostatic dielectric calculations and time-resolved measurements of solvation dynamics and ET kinetics posed in Sec. II C. The predominant contribution of the k integral including $S^L(k)$ to λ_s should lead to longitudinal dynamics when $S^L(k)$ is replaced by $S^L(k,\omega)$ to extend the NRFT to time-dependent phenomena.

It would be, however, wrong to assume that the transverse response and transverse component of the field of the ET dipole do not affect λ_s. The role of the transverse response is to change the weight with which the longitudinal structure factor affects the solvation thermodynamics. In case of a purely longitudinal electric field of the solute, λ_p includes only the longitudinal component λ^L [Eq. (84)]. For a dipolar solute, the existence of a transverse component in the solute field leads to the appearance of a factor of about 1.5 in front of the longitudinal reorganization energy [Eq. (104)]. In the case of a solute of arbitrary shape, the mean-field solution produces an effective electric field, including both the longitudinal and transverse components of $\Delta\tilde{\mathbf{E}}_0$, which couples to the longitudinal structure factor [Eq. (110)]. This alteration of the longitudinal field becomes less important with increasing separation between the positive and negative ends in the ET dipole. It turns out to be insignificant for the contact DAC diatomic as is seen by comparing the line labeled λ^L with the dotted line in Fig. 16.

The longitudinal component of λ_p shows some interesting peculiarities. The dot-dashed line labeled "L" in Fig. 16 indicates the continuum limit for the longitudinal component of λ_s^{MF} [Eq. (110)] obtained by setting $S^L(k)=S^L(0)$. The dash-dotted line labeled "T" shows the continuum limit for the transverse component of λ_p^{MF}. The gap between the con-

tinuum limit labeled as "L+T" and the full microscopic calculation (solid line labeled "λ_p") arises from the dependence of the solvent response function on the wave vector k neglected in the continuum limit. Note that for equal definitions of the solute excluded volume (cavity) the following inequality holds between the macroscopic and microscopic values of the longitudinal reorganization energy:

$$\lambda_s^{\mathrm{M}} < \lambda_s^L, \tag{129}$$

where λ_s^{M} is given by Eq. (1). The above inequality is related to the property of the longitudinal polarization structure factor: $S^L(k) \geqslant S^L(0)$. One of the consequences of a significant dependence of λ_p on the microscopic, k-dependent part of the response function is that it is fundamentally impossible to define the "best" cavity for continuum calculations which would not depend on the solvent identity and the ratio of characteristic dimensions of the solute and the solvent molecules.

The length of decay of $S^T(k)$ in polar liquids should be compared to the length of decay of the fields $k^2|\Delta\tilde{E}_0^L|^2$ and $k^2|\Delta\tilde{E}_0^T|^2$ entering the one-dimensional k integrals in Eqs. (84) and (110). Only if the decay of the field is faster than the decay of $S^T(k)$ can one use the continuum assumption $S^T(k) \simeq S^T(0)$, resulting in the continuum formulas for the solvation thermodynamics. The longitudinal structure factor does not change as strongly as does the transverse structure factor at small k values, and the condition $S^T(k) \simeq S^T(0)$ guarantees a similar condition $S^L(k) \simeq S^L(0)$ for the longitudinal structure factor. This observation allows us to formulate a quantitative criterion for the applicability of continuum models. Over several decades of active application of continuum calculations,[50] it has always been assumed that the solute should be sufficiently larger than the solvent for this approach to be applicable. Exactly how much larger has remained an open question.

It is clear from the above discussion that a criterion for continuum models applicability will depend on the multipolar symmetry of the solute field (e.g., charge or dipole) as well as on the size and polarity of the solvent molecules. One can define the characteristic length of the field decay as the value k_0 at which $k^2|\Delta\tilde{E}_0^L|^2$ and $k^2|\Delta\tilde{E}_0^T|^2$ reach their first $k \neq 0$ zero. For a spherical ion of radius R_0, $k_0 = \pi/R_0$ [first zero of $j_0(x)$], whereas for a spherical dipole, $k_0 \simeq 4.49/R_0$ [second zero of $j_1(x)$]. The length k_0 should be compared to the length of decay of $S^T(k)$ for which we will take the distance $k_{1/2}$ such that $S^T(k_{1/2}) - 1 = [S^T(0) - 1]/2$ (see Fig. 15). The criterion for the validity of continuum models then becomes

$$R_0 \gg R_{\mathrm{mult}} = \frac{a_{\mathrm{mult}}}{k_{1/2}}, \tag{130}$$

where $a_{\mathrm{mult}} = \pi$ for ions and $a_{\mathrm{mult}} = 4.49$ for dipoles. Figure 17 shows the dependence of R_{mult} on the solvent dielectric constant calculated for ionic (lower curve) and dipolar (upper curve) solutes. The calculations are performed by changing the dipolar density y of a nonpolarizable solvent with dielectric constant calculated according to Eq. (102) and $S^T(k)$ obtained from the PPST. As expected, the criterion of applicability of continuum models is more stringent for dipolar solutes compared to ionic solutes. The solute size required for the continuum approximation to be applicable turns out to be fairly large: for water with $\sigma = 2.87$ Å and $\epsilon_s = 78$ one should require the radius of ionic and dipolar solutes to be significantly larger than 8.6 and 12.5 Å, respectively. When criterion (130) holds, one can apply the Poisson equation to calculate the solvation free energy. When it does not hold, the transverse component in the Poisson solution is irrelevant and a useful continuum approximation is to combine longitudinal solvation with the vdW cavity (labeled vdW/L in Figs. 9 and 10).

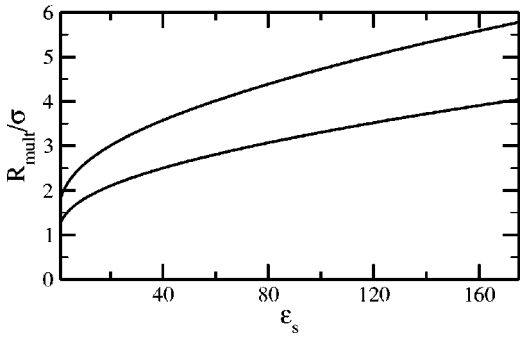

FIG. 17. R_{mult} from Eq. (130) vs ϵ_s calculated for a nonpolarizable dipolar solvent using Eq. (102) and the PPST. The upper and lower curves refer to a dipolar and ionic spherical solutes, respectively.

The NRFT provides new insights into the dependence of the solvent reorganization energy on solvent's high-frequency dielectric constant ϵ_∞. Since no extensive simulation or experimental studies of this problem have been performed so far, the following discussion should be considered as a *prediction* of the microscopic theory. In Sec. IV A we have already alluded to the fact that the NRFT results in a very weak dependence of the reorganization energy λ_p on ϵ_∞. Figure 18 shows λ_p from the mean-field solution [Eq. (110)] versus ϵ_∞ obtained for a contact DA diatomic. As in the case of the exact solution for a dipolar solute (Fig. 12) the microscopic result for λ_p is almost insensitive to ϵ_∞ (solid line in Fig. 18). The transition to the continuum limit in the microscopic equations by neglecting the k dependence of the polarization structure factors leads to a very pro-

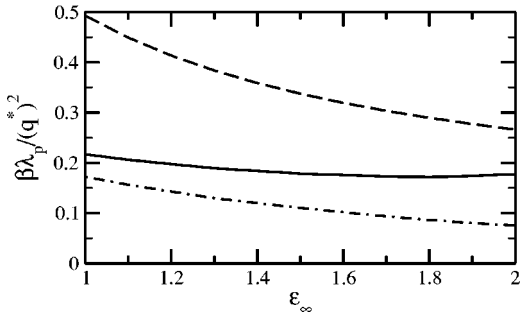

FIG. 18. λ_p vs ϵ_∞ for a contact diatomic calculated from the NRFT [Eq. (110), solid line], its continuum limit obtained by neglecting the k dependence in the polarization structure factors (dot-dashed line), and from the Marcus equation [Eq. (38), dashed line]. The molecular solvent polarizability at each magnitude of ϵ_∞ is calculated from the Clausius–Mossotti equation and the static dielectric constant from Eq. (102); $(m^*)^2 = 1.0$, $\rho^* = 0.8$, $R_0/\sigma = 0.9$, and $R/\sigma = 1.8$.

nounced dependence on ϵ_∞ (dot-dashed line in Fig. 18) which parallels the dependence on ϵ_∞ of the Marcus equation [Eq. (38), dashed line in Fig. 18]. In fact, the falloff of the reorganization energy by about a factor of 2 when ϵ_∞ changes from 1 to 2 in polar solvents predicted by the Marcus equation is almost exactly reproduced by the continuum limit of the microscopic formulation. Therefore, if the prediction of a nearly independence of λ_p of ϵ_∞ is supported by computer simulations, it would imply that using continuum models for solutes which do not comply with criterion (130) results, among other problems, in a too strong dependence of the reorganization energy on ϵ_∞ (Ref. 124). This fact can also make the longitudinal reorganization energy, which is close to simulations in nonpolarizable solvents (Figs. 9 and 10), too low when the strong dependence on ϵ_∞ is incorporated in the continuum solution. On the other hand, the Poisson/vdW solution, which is too high in nonpolar solvents, may fall to a reasonable value at $\epsilon_\infty > 1$ as a result of cancellation of errors.

The Gaussian analysis of the distribution of donor–acceptor energy gaps embodied in the Marcus–Hush theory of ET introduces two parameters to the model: the average vertical energy gap $\langle \Delta E \rangle$ and the variance $\sigma(\Delta E)^2$ (Fig. 3). The traditional formulation splits $\langle \Delta E \rangle$ into the driving force ΔF_0 and the reorganization energy λ_s and gives $\sigma(\Delta E)^2$ as a product of $2k_BT$ and λ_s [Eq. (9)]. Variance $\sigma(\Delta E)^2$ is caused by thermal noise of the electrostatic potential of the solvent at locations of solute charges. Thermal fluctuations of the solvent can be broadly subdivided into angular-independent and angular-dependent fluctuations. This corresponds to splitting of $\sigma(\Delta E)^2$ into the spherically symmetric component $\sigma_d(\Delta E)^2 = 2k_BT\lambda_d$ and an angular-dependent component $\sigma_p(\Delta E)^2 = 2k_BT\lambda_p$. The latter splits into the longitudinal and transverse contributions according to the symmetry of the charge–dipole solute–solvent interaction potential. The final result for the variance of the donor–acceptor gap is

$$\sigma(\Delta E)^2 = \sigma_d(\Delta E)^2 + \sigma_p^L(\Delta E)^2 + \sigma_p^T(\Delta E)^2. \tag{131}$$

The splitting of the variance is based on the symmetry and not on actual physical modes—molecular translations and rotations—contributing to the thermal noise. For example, molecular translations may contribute to both the polarization structure factors and density structure factor. However, the common physical understanding of these two types of structure factors predominantly attributes molecular translations to the density structure factor and molecular rotations to the polarization structure factors.[125] Based on this attribution, the splitting of $\sigma(\Delta E)^2$ into "d" and "p" components should approximately reflect corresponding weights of translational and rotational modes in the statistics of donor–acceptor gap fluctuations.

As discussed above, the transverse component is insignificant in Eq. (131). The longitudinal reorganization energy λ^L does not contain an explicit dependence on temperature because of the cancellation of the y_p factor by chain contributions of long-range dipole–dipole forces (Sec. II E). As a result, the longitudinal component of the variance is proportional to T, $\sigma_p^L(\Delta E)^2 \propto T$. On the contrary, the cancellation of y_p does not happen for λ_d and $\lambda_d \propto y_p$, resulting in $\sigma_d(\Delta E)^2$ which does not have any explicit dependence on temperature. The overall explicit dependence of $\sigma(\Delta E)^2$ on T has the form

$$\sigma(\Delta E)^2 = a + bT, \tag{132}$$

where a and b depend on T implicitly, through solvent parameters. The use of this type of variance in the Gaussian form for the resonance probability $P_i(0)$ [Eq. (8)] leads to a non-Arrhenius form for the ET rate constant:

$$k_{\mathrm{ET}} \propto \exp\left[-\frac{\langle \Delta E \rangle^2}{2a + 2bT} \right]. \tag{133}$$

This result indicates that the macroscopic fluctuation–dissipation theorem breaks down for short-range, molecular-scale fluctuations. The description of the entropy of activation is thus sensitive to molecular details of solute–solvent interaction.[42] The non-Arrhenius character of ET kinetics should become more pronounced in solvents with a microscopic length of fluctuations where cancellation of the multipolar density factor [y_p for dipoles and $y_q = (2\pi/5)\rho\beta Q^2/\sigma^2$ for axial quadrupoles Q (Ref. 36)] is not as effective as for dipolar solvents; ET in quadrupolar solvents is an example.[126] One should note that the fluctuation–dissipation theorem is not expected to hold for solvent density fluctuations. They modulate the linear coupling of the solute field to the solvent polarization in a nonlinear fashion, thus violating the assumption of linear coupling between a weak external field and a solvent mode explicitly used in the derivation of the theorem.[96]

VII. SUMMARY

This paper presents an analytical formalism for the calculation of the solvent reorganization energy of ET in a solute of arbitrary shape and arbitrary charge distribution. The formalism is realized in a computational algorithm which allows us to study ET in large molecules of the size of biopolymers[127] with a computational cost comparable to that of dielectric continuum calculations. The results of calculations on model ET systems agree well with MC simulations. The theory highlights the difference in the mechanisms of ET activation by longitudinal and transverse polarization modes and by local density fluctuations of the solvent. From a broader perspective, the present formulation indicates that the concept of longitudinal polarization embodied in the Born theory of ionic solvation[3] and Marcus theory of ET activation[79] is correct for small- and medium-size solutes. The more mathematically elaborate description due to Onsager[71] solves the Poisson equation and incorporates both longitudinal and transverse polarization modes into the solvation free energy. This solution applies to large solutes with the effective radius greater than about four solvent diameters. There is, however, no continuum approximation which would incorporate both the Born and Onsager pictures in one formalism.

ACKNOWLEDGMENTS

Acknowledgments are made to the Donors of The Petroleum Research Fund, administered by the American Chemical Society (Grant No. 39539-AC6), for support of this research. The author is grateful to Dr. M. S. Skaf for sharing results of his simulations and to Dr. M. D. Newton for critical comments on the manuscript. This is publication 573 from the ASU Photosynthesis Center.

APPENDIX A: MC SIMULATIONS

MC simulations have been carried out in two basic setups: simulations of the pure dipolar–quadrupolar solvents and simulations of solvation. The goal of simulating pure solvents was to obtain dielectric properties for the comparison of the analytical theory and simulations to the predictions of the dielectric continuum theory and to calculate polarization and density structure factors used to test the PPSF. The MC protocol employed $N=500$ and 864 solvent molecules in a cubic simulation box with the reaction-field correction for the cutoff of the long-ranged dipolar and quadrupolar forces.[128] For dipolar–quadrupolar liquids, axial quadrupoles were employed. This means that the molecular quadrupolar matrix is diagonal in coordinates with a principle axes in the direction of the solvent dipole. The dipole and quadrupole moment were characterized by their reduced values: $(m^*)^2=\beta m^2/\sigma^3$ and $(Q^*)^2=\beta Q^2/\sigma^5$. The dielectric properties of dipolar and dipolar–quadrupolar solvents obtained from simulations are listed in Table I.

Solvation simulations included several configurations of the DAC. Testing of the LRA for dipolar solvation in dipolar and quadrupolar solvents was carried out for a spherical solute of the radius $R_0=0.9\sigma$ with varying dipole moment. The solute–solvent potential was calculated with the reaction-field correction for the long-distance cutoff.[128] The solute was immobilized at the center of a cubic simulation box containing 500 solvent molecules at the reduced density $\rho^*=0.8$.

Ewald-sum calculation[128] of the solute-solvent potential was used for simulations of diatomic solutes. In the neutral state, the variance of the solute–solvent interaction potential was taken on solvent configurations in equilibrium with a neutral hard-core solute with $R_A=R_D=0.9\sigma$. The contact configuration $R=2R_D$ was adopted for simulation results presented in Figs. 4, 8, and 9. For the simulations of the distance dependence of λ_s the interval of distances $1.8\sigma \leqslant R \leqslant 3\sigma$ was explored. In the charged state of the donor–acceptor diatomics, simulations were performed with the explicit account for the interaction of solvent dipoles with the solute charges z_i:

$$\beta v_2(j)=-q^*m^*\sigma^2\sum_{i=1,2} z_i\frac{\hat{\mathbf{m}}_j\cdot\hat{\mathbf{r}}_j}{r_j^2}, \tag{A1}$$

where the reduced charge is

$$(q^*)^2=\beta e^2/\sigma. \tag{A2}$$

Opposite charges with the magnitude $q^*=11.87$ were placed on the donor and acceptor. The simulation results for the reorganization energies and their splitting into the one-molecule and two-molecule components are listed in Table II.

TABLE I. Simulations of dielectric parameters for pure dipolar liquids $[(Q^*)^2=0]$ and dipolar liquids with axial quadrupole moments $[(Q^*)^2=0.5]$ at different reduced solvent dipole moments $(m^*)^2=\beta m^2/\sigma^3$. MC simulations were carried out for fluids of $N=500$ and 864 molecules in a cubic simulation box with the reaction-field cutoff of the multipole interactions; the length of each simulation is 1.4×10^6 cycles.

	$(Q^*)^2=0$			$(Q^*)^2=0.5$		
$(m^*)^2$	g_K	ϵ_s	$S^T(0)$	g_K	ϵ_s	$S^T(0)$
0.5	1.24	3.74	1.64	0.91	2.94	1.16
1.0	1.62	8.7	2.29	0.95	5.34	1.30
1.5	2.15	16.7	3.12	1.04	8.42	1.48
2.0	2.94	30.1	4.34	1.20	12.6	1.73
2.5	4.25	54.0	6.32	1.27	16.5	1.84
3.0	5.94	90.1	8.86	1.46	22.6	2.14
3.5	10.4	184	15.6	1.61	28.8	2.37
4.0	18.4	371	27.6	1.81	36.9	2.68

TABLE II. Reorganization energy $\beta\lambda_s/(q^*)^2$ (I) and its splitting into the one-molecule, $\beta\lambda_s^{\mathrm{I}}/(q^*)^2$ (II), and two-molecule, $\beta\lambda_s^{\mathrm{II}}/(q^*)^2$ (III), components at changing solvent dipolar strength $(m^*)^2=\beta m^2/\sigma^3$. The simulations are carried out for a neutral solute diatomic (D–A) in dipolar and dipolar–quadrupolar solvents and for a charged diatomic (D^+-A^-) in dipolar solvents. The solute is modeled by two spheres of the radius $R_A=R_D=0.9\sigma$ at the distance $R=R_D+R_A$; $\rho^*=0.8$ and $q^*=11.87$.

	D–A, $(Q^*)^2=0$			D–A, $(Q^*)^2=0.5$			D^+-A^-, $(Q^*)^2=0$		
$(m^*)^2$	I	II	III	I	II	III	I	II	III
0.5	0.241	0.457	−0.216	0.247	0.440	−0.193	0.234	0.502	−0.268
1.0	0.325	0.899	−0.574	0.357	0.881	−0.524	0.316	0.990	−0.674
1.5	0.368	1.328	−0.960	0.406	1.312	−0.906	0.361	1.461	−1.100
2.0	0.389	1.743	−1.354	0.450	1.726	−1.276	0.389	1.913	−1.524
2.5	0.399	2.111	−1.712	0.472	2.117	−1.645	0.403	2.356	−1.953
3.0	0.420	2.490	−2.070	0.475	2.530	−2.055	0.423	2.779	−2.356
3.5	0.426	2.837	−2.411	0.495	2.894	−2.399	0.438	3.180	−2.742
4.0	0.430	3.146	−2.716	0.511	3.219	−2.708	0.448	3.566	−3.118
4.5	0.433	3.456	−3.023	0.516	3.450	−2.934	0.452	3.922	−3.470
5.0	0.425	3.685	−3.260	0.522	3.772	−3.250	0.511	4.734	−4.223
6.0	0.435	4.238	−3.803	0.494	4.823	−4.329	0.474	4.650	−4.176

APPENDIX B: NOTATION USED FOR DIRECT AND INVERTED SPACE INTEGRATION

The following notation is accepted for direct- and inverted-space integrals. Two functions combined with the asterisk denote integration over the direct-space coordinates:

$$v*u=\int v(\mathbf{r})u(\mathbf{r})d\mathbf{r}. \tag{B1}$$

The combination of three functions separated by asterisks denotes convolution:

$$v*f*u=\int v(\mathbf{r}_1)f(\mathbf{r}_1-\mathbf{r}_2)u(\mathbf{r}_2)d\mathbf{r}_1d\mathbf{r}_2. \tag{B2}$$

Fourier transforms are denoted by tildas and the corresponding asterisks product is defined as

$$\tilde{v}*\tilde{u}=\int \tilde{v}(\mathbf{k})\tilde{u}(\mathbf{k})[d\mathbf{k}/(2\pi)^3]. \tag{B3}$$

The interaction potentials and correlation functions depending on the orientations of solvent dipoles are indicated by using indexes 1, 2,... standing for orientations of the corresponding dipole moments ω_1, ω_2,.... The k-space convolution then becomes

$$\tilde{v}*\tilde{f}*\tilde{v}=\int \tilde{v}(\mathbf{k}_1,\omega_1)\tilde{f}(\mathbf{k}_1-\mathbf{k}_2,\omega_1,\omega_2)\tilde{v}(\mathbf{k}_2,\omega_2) \times\frac{d\mathbf{k}_1d\mathbf{k}_2}{(2\pi)^6}\frac{d\omega_1d\omega_2}{(4\pi)^2}. \tag{B4}$$

APPENDIX C: FOURIER TRANSFORM OF THE FIELD OF ET DIPOLE

To avoid numerical divergence of the Fourier integral in Eq. (3), the solvent is represented by a sum of Fourier transforms over two volumes Ω_1 and Ω_2 which together make the solvent volume Ω (Fig. 19). The total difference field is then a sum of Fourier transforms from each region,

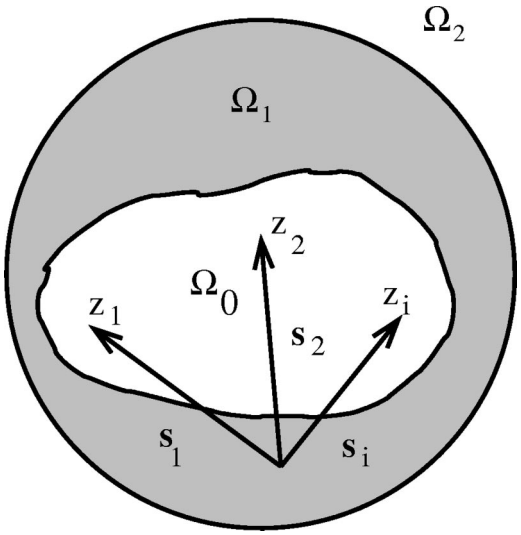

FIG. 19. Donor–acceptor complex occupying the region of space Ω_0 with charges z_i located at $\mathbf{s}_i$. The shaded area is Ω_1, and the area outside the sphere encircling the DAC is Ω_2.

$$\Delta\tilde{\mathbf{E}}_0=\Delta\tilde{\mathbf{E}}_0(\Omega_1)+\Delta\tilde{\mathbf{E}}_0(\Omega_2). \tag{C1}$$

The first summand in Eq. (C1) is calculated numerically by the FFT,[123] and the second summand is calculated analytically for an arbitrary distribution of charges z_i with the coordinates $\mathbf{s}_i$, $s_i<L$ (Fig. 19):

$$\Delta\tilde{\mathbf{E}}_0(\Omega_2)=-4\pi e\sum_i z_i\sum_{n=1}^{\infty}(-i)^n\left(\frac{s_i}{L}\right)^{n-1} \times\frac{j_{n-1}(kL)}{k}[\hat{\mathbf{s}}_iP'_{n-1}(\cos\theta_i)-\hat{\mathbf{k}}P'_n(\cos\theta_i)]. \tag{C2}$$

Here $\cos\theta_i=\hat{\mathbf{s}}_i\cdot\hat{\mathbf{k}}$ and L is the radius of the sphere enclosing the volume Ω_1 (Fig. 19), $j_n(x)$ is the spherical Bessel function, and $P_n(\cos\theta_i)$ is the Legendre polynomial.

[1] R. A. Marcus, J. Chem. Phys. **24**, 966 (1956).
[2] R. A. Marcus, J. Chem. Phys. **43**, 679 (1965).
[3] M. Born, Z. Phys. **1**, 45 (1920).
[4] S. I. Pekar, *Research in Electron Theory of Crystals* (USAEC, Washington, D.C., 1963).
[5] L. D. Zusman, Chem. Phys. **49**, 295 (1980).
[6] B. Bagchi and A. Chandra, Adv. Chem. Phys. **80**, 1 (1991).
[7] H. Heitele, Angew. Chem., Int. Ed. Engl. **32**, 359 (1993).
[8] P. V. Kumar and M. Maroncelli, J. Chem. Phys. **103**, 3038 (1995).
[9] G. van der Zwan and J. T. Hynes, J. Phys. Chem. **89**, 4181 (1985).
[10] P. F. Barbara and W. Jarzeba, Adv. Photochem. **15**, 1 (1990).
[11] P. Madden and D. Kivelson, Adv. Chem. Phys. **56**, 467 (1984).
[12] M. Neumann, Mol. Phys. **57**, 97 (1986).
[13] Y. I. Kharkats, A. A. Kornishev, and M. A. Vorotyntsev, J. Chem. Soc., Faraday Trans. 2 **72**, 361 (1976).
[14] C. J. F. Böttcher, *Theory of Electric Polarization* (Elsevier, New York, 1973).
[15] E. D. German and A. M. Kuznetsov, Electrochim. Acta **26**, 1595 (1981).
[16] Y.-P. Liu and M. D. Newton, J. Phys. Chem. **98**, 7162 (1994).
[17] K. A. Sharp, Biophys. J. **73**, 1241 (1998).
[18] B. S. Brunschwig, S. Ehrenson, and N. Sutin, J. Phys. Chem. **90**, 3657 (1986).
[19] Y. Zhou, H. L. Friedman, and G. Stell, Chem. Phys. **152**, 185 (1991).
[20] D. V. Matyushov, Chem. Phys. **174**, 199 (1993).
[21] B.-C. Perng, M. D. Newton, F. O. Raineri, and H. L. Friedman, J. Chem. Phys. **104**, 7153 (1996).
[22] F. O. Raineri and H. L. Friedman, Adv. Chem. Phys. **107**, 81 (1999).
[23] T. Fonseca, B. M. Ladanyi, and J. T. Hynes, J. Phys. Chem. **96**, 4085 (1992).
[24] S.-H. Chong, S. Miura, G. Basu, and F. Hirata, J. Phys. Chem. **99**, 10526 (1995).
[25] E. A. Carter and J. T. Hynes, J. Chem. Phys. **94**, 5961 (1991).
[26] J.-K. Hwang and A. Warshel, J. Am. Chem. Soc. **109**, 715 (1987).
[27] R. A. Kuharski, J. S. Bader, D. Chandler, M. Sprik, M. L. Klein, and R. W. Impey, J. Chem. Phys. **89**, 3248 (1988).
[28] L. W. Ungar, M. D. Newton, and G. A. Voth, J. Phys. Chem. B **103**, 7367 (1999).
[29] B.-C. Perng, M. D. Newton, F. O. Raineri, and H. L. Friedman, J. Chem. Phys. **104**, 7177 (1996).
[30] D. V. Matyushov and M. D. Newton, J. Phys. Chem. A **105**, 8516 (2001).
[31] T. Ichiye, J. Chem. Phys. **104**, 7561 (1996).
[32] D. V. Matyushov, Mol. Phys. **79**, 795 (1993).
[33] B. M. Ladanyi and R. M. Stratt, J. Phys. Chem. **100**, 1266 (1996).
[34] R. Biswas, N. Nandi, and B. Bagchi, J. Phys. Chem. B **101**, 2968 (1997).
[35] L. Reynolds, J. A. Gardecki, S. J. V. Frankland, and M. Maroncelli, J. Phys. Chem. **100**, 10337 (1996).
[36] D. V. Matyushov and G. A. Voth, J. Chem. Phys. **111**, 3630 (1999).
[37] I. Read, A. Napper, M. B. Zimmt, and D. H. Waldeck, J. Phys. Chem. A **104**, 9385 (2000).
[38] D. V. Matyushov and R. Schmid, Mol. Phys. **84**, 533 (1995).
[39] D. V. Matyushov and R. Schmid, J. Chem. Phys. **103**, 2034 (1995).
[40] D. L. Derr and C. M. Elliott, J. Phys. Chem. A **103**, 7888 (1999).

[41] S. F. Nelsen, R. F. Ismagilov, K. E. Gentile, and D. R. Powell, J. Am. Chem. Soc. **121**, 7108 (1999).
[42] P. Vath, M. B. Zimmt, D. V. Matyushov, and G. A. Voth, J. Phys. Chem. B **103**, 9130 (1999).
[43] P. Vath and M. B. Zimmt, J. Phys. Chem. A **104**, 2626 (2000).
[44] X. Zhao, J. A. Burt, F. J. Knorr, and J. L. McHale, J. Phys. Chem. A **105**, 11110 (2001).
[45] G. Stell, G. N. Patey, and J. S. Høye, Adv. Chem. Phys. **18**, 183 (1981).
[46] A. Milischuk and D. V. Matyushov, J. Chem. Phys. **118**, 1859 (2003).
[47] D. V. Matyushov and B. M. Ladanyi, J. Chem. Phys. **110**, 994 (1999).
[48] A. M. Napper, I. Read, R. Kaplan, M. B. Zimmt, and D. H. Waldeck, J. Phys. Chem. A **106**, 5288 (2002).
[49] F. Raineri and H. Friedman, J. Chem. Phys. **98**, 8910 (1993).
[50] C. J. Cramer and D. G. Truhlar, Chem. Rev. (Washington, D.C.) **99**, 2161 (1999).
[51] R. M. Lynden-Bell, AIP Conf. Proc. **492**, 3 (1999).
[52] B. M. Ladanyi and M. S. Skaf, Annu. Rev. Phys. Chem. **44**, 335 (1993).
[53] L. R. Pratt and D. Chandler, J. Chem. Phys. **67**, 3683 (1977).
[54] D. Chandler, Phys. Rev. E **48**, 2898 (1993).
[55] X. Song, D. Chandler, and R. A. Marcus, J. Phys. Chem. **100**, 11954 (1996).
[56] X. Song and D. Chandler, J. Chem. Phys. **108**, 2594 (1998).
[57] C. G. Gray and K. E. Gubbins, *Theory of Molecular Liquids* (Clarendon, Oxford, 1984).
[58] F. O. Raineri, H. Resat, and H. L. Friedman, J. Chem. Phys. **96**, 3068 (1992).
[59] M. S. Skaf, J. Chem. Phys. **107**, 7996 (1997).
[60] D. Ben-Amotz and D. R. Herschbach, J. Phys. Chem. **90**, 1038 (1990).
[61] D. Ben-Amotz and K. G. Willis, J. Phys. Chem. **97**, 7736 (1993).
[62] R. Schmid and D. V. Matyushov, J. Phys. Chem. **99**, 2393 (1995).
[63] D. V. Matyushov and R. Schmid, J. Chem. Phys. **105**, 4729 (1996).
[64] S. W. Rick and S. J. Stuart, *Reviews in Computational Chemistry* (Wiley-VCH, New York, 2002), Vol. 18, p. 89.
[65] S. Gupta and D. V. Matyushov, J. Phys. Chem. A **108**, ASAP (2004).
[66] M. S. Wertheim, Mol. Phys. **37**, 83 (1979).
[67] V. Venkatasubramanian, K. E. Gubbins, C. G. Gray, and C. C. Joslin, Mol. Phys. **52**, 1411 (1984).
[68] C. G. Joslin, C. G. Gray, and K. E. Gubbins, Mol. Phys. **54**, 1117 (1985).
[69] D. Ben-Amotz and I. P. Omelyan, J. Chem. Phys. **115**, 9401 (2001).
[70] M. B. Zimmt and D. H. Waldeck, J. Phys. Chem. A **107**, 3580 (2003).
[71] L. Onsager, J. Am. Chem. Soc. **58**, 1486 (1936).
[72] J. G. Kirkwood, J. Chem. Phys. **2**, 351 (1934).
[73] R. H. Wood, J. R. Qulnt, and J.-P. E. Groller, J. Phys. Chem. **85**, 3944 (1981).
[74] M. Berg, J. Phys. Chem. A **102**, 17 (1998).
[75] J. Jeon and H. J. Kim, J. Chem. Phys. **119**, 8606 (2003).
[76] R. A. Marcus, J. Phys. Chem. **93**, 3078 (1989).
[77] C. H. Wang, *Spectroscopy of Condensed Media* (Academic, Orlando, FL, 1985).
[78] B. M. Ladanyi and M. Maroncelli, J. Chem. Phys. **109**, 3204 (1998).
[79] R. A. Marcus, Rev. Mod. Phys. **65**, 599 (1993).
[80] D. V. Matyushov and G. A. Voth, J. Chem. Phys. **113**, 5413 (1999).
[81] A. Milischuk and D. V. Matyushov, J. Phys. Chem. A **106**, 2146 (2002).
[82] The solvent reorganization energy is defined as the equilibrium free energy of solvation of the ET dipole. The approach used here can be applied to a DAC with an arbitrary charge as long as the solute charge does not change the spectrum of fluctuations of the solvent (LRA).
[83] M. S. Wertheim, J. Chem. Phys. **55**, 4291 (1971).
[84] D. Y. C. Chan, D. J. Mitchell, and B. W. Ninham, J. Chem. Phys. **70**, 2946 (1979).
[85] J. S. Høye and G. Stell, J. Chem. Phys. **73**, 461 (1980).
[86] H. E. Stanley, *Introduction to Phase Transitions and Critical Phenomena* (Oxford University Press, New York, 1987).
[87] The charges of the solute interact only with optical phonons changing the local charge distribution in the solvent. Therefore thermal excitations, leading to a parallel tilt of the dipoles, can be neglected.
[88] J. P. Hansen and I. R. McDonald, *Theory of Simple Liquids* (Academic, Orlando, FL, 1986).
[89] J. T. Hupp, Y. Dong, R. L. Blackbourn, and H. Lu, J. Phys. Chem. **97**, 3278 (1993).
[90] W. Rocchia, E. Alexov, and B. Honig, J. Phys. Chem. B **105**, 6507 (2001).
[91] W. Rocchia, S. Sridharan, A. Nicholls, E. Alexov, A. Chiabrera, and B. Honig, J. Comput. Chem. **23**, 128 (2002).
[92] B. Berne, J. Chem. Phys. **62**, 1154 (1975).
[93] A. Chandra, D. Wei, and G. N. Patey, J. Chem. Phys. **99**, 4926 (1993).
[94] B. Bagchi and N. Gayathri, in *Advances in Chemical Physics*, edited by J. Jortner and M. Bixon (Wiley, New York, 1999), Vol. 107, p. 1.
[95] A. A. Ovchinnikov and M. Y. Ovchinnikova, Sov. Phys. JETP **29**, 688 (1969).
[96] R. Kubo, *Lectures in Theoretical Physics* (Interscience, New York, 1959), Vol. 1, p. 120.
[97] H. C. Andersen and D. Chandler, J. Chem. Phys. **57**, 1918 (1972).
[98] J. S. Høye and G. Stell, J. Chem. Phys. **61**, 562 (1974).
[99] Short-range and long-range interactions can be distinguished based on the convergence property of the second virial coefficient. The latter diverges for radial interaction potentials $\propto 1/r^{\delta}$ at $\delta \leqslant 3$ (long-range potential) and is finite at $\delta > 3$ (short-range potential).
[100] N. Mataga, *Molecular Interactions and Electronic Spectra* (Dekker, New York, 1970).
[101] M. S. Skaf and B. M. Ladanyi, J. Chem. Phys. **102**, 6542 (1995).
[102] P. A. Bopp, A. A. Kornyshev, and G. Sutmann, Phys. Rev. Lett. **76**, 1280 (1996).
[103] B.-C. Perng and B. M. Ladanyi, J. Chem. Phys. **110**, 6389 (1999).
[104] I. P. Omelyan, Mol. Phys. **93**, 123 (1998).
[105] M. Lilichenko and D. V. Matyushov, J. Chem. Phys. **119**, 1559 (2003).
[106] D. V. Matyushov and G. A. Voth, J. Phys. Chem. A **103**, 10981 (1999).
[107] J. Richardi and P. H. Fries, J. Mol. Liq. **88**, 209 (2000).
[108] D. V. Matyushov and B. M. Ladanyi, J. Chem. Phys. **108**, 6362 (1998).
[109] G. Fischer, *Vibronic Coupling* (Academic, London, 1984).
[110] J. S. Høye and G. Stell, J. Chem. Phys. **64**, 1952 (1976).
[111] L. R. Pratt, Mol. Phys. **40**, 347 (1980).
[112] M. J. Thompson, K. S. Schweizer, and D. Chandler, J. Chem. Phys. **76**, 1128 (1982).
[113] J. Cao and B. J. Berne, J. Chem. Phys. **99**, 2902 (1993).
[114] E. L. Pollock, B. J. Alder, and G. N. Patey, Physica A **108**, 14 (1981).
[115] H. Li and M. Kardar, Phys. Rev. A **46**, 6490 (1992).
[116] D. V. Matyushov, J. Chem. Phys. **120**, 1375 (2004).
[117] A singularity of the integrand in Eq. (95) in fact appears at k^* defined by the condition $S^L + 2A = 0$. This pole is responsible for longitudinal polarization waves generated in a polar solvent by the insertion of the solute. However, this singularity gives a negligible contribution to the integral and is not considered here.
[118] A. Tani, D. Henderson, and J. A. Barker, Mol. Phys. **48**, 863 (1983).
[119] J. S. Bader and B. J. Berne, J. Chem. Phys. **104**, 1293 (1996).
[120] P. J. Rossky and B. M. Pettitt, Mol. Phys. **50**, 1263 (1983).
[121] R. J. Baxter, J. Chem. Phys. **52**, 4559 (1970).
[122] The effective HS diameter of DMSO calculated by fitting the solvent compressibility to that given by the generalized van der Waals equation is 4.95 Å. The compressibility of the ISM fluid used to represent DMSO may be, however, different from the compressibility of the real solvent.
[123] W. H. Press, S. A. Teukolsky, W. T. Vetterling, and B. P. Flannery, *Numerical Recipes in Fortran 77: The art of scientific computing* (Cambridge University Press, Cambridge, England, 1996).
[124] A strong dependence on ϵ_∞ will appear in any theory of ET reorganization that implements an additive correction for electronic polarizability effects not entangled with the nonlocal response functions. For instance, the RISM formulation in Ref. 29 relies on an additive correction the dependence on ϵ_∞ in which is as strong as in the Marcus formula.
[125] H. L. Friedman, *A Course in Statistical Mechanics* (Prentice-Hall, Englewood Cliffs, NJ, 1985).
[126] I. Read, R. Kaplan, M. B. Zimmt, and D. H. Waldeck, J. Am. Chem. Soc. **121**, 10976 (1999).
[127] D. N. LeBard, M. Lilichenko, D. V. Matyushov, Y. A. Berlin, and M. A. Ratner, J. Phys. Chem. B **107**, 14509 (2003).
[128] M. P. Allen and D. J. Tildesley, *Computer Simulation of Liquids* (Clarendon, Oxford, 1996).